CONSTRUCTION MATERIALS CONSULTANTS, INC.

Assessment of Concrete Inside A Train Shed From The Grand Central Terminal In The City Of New York

Rehabilitation of the Grand Central Terminal Train Shed – Sector 2 (53/55 St)
Park Avenue between 53rd and 55th St.
New York, New York

September 9, 2021
CMC 0821148

TABLE OF CONTENTS

EXECUTIVE SUMMARY

The present investigation centered around assessment of compositions, qualities, and conditions of concretes in seven (7) concrete cores retrieved from the walls on train tracks in the enclosed shaded area under Park Avenue between 53rd and 55th Street in the Grand Central Terminal, Sector 2 in New York, New York. Original concrete construction is reported to be circa 1910 - 1920 with miscellaneous repairs and rehabilitation projects since then. Due to its presence in a protected environment, i.e., not exposed to the elements of the harsh outdoor environment of New York city, concrete at the locations of the cores examined are reportedly present in reasonably 'mild' conditions given its age without any visible distress.

Selected portions of seven (7) cores out of a total seventeen (17) cores retrieved were provided for detailed petrographic examinations of two (2) cores, air-void analysis of two (2) other cores, and water-soluble chloride and sulfate analyses of five (5) cores at two different depths for each core. Additionally, results of compressive strength tests of all seventeen (17) cores were provided.

Based on comprehensive laboratory studies, concretes across the cores examined as well as not examined (i.e., except only examining the photos of full-length cores provided) showed some similarities as well as differences in the concretes delivered to the core locations, which may indicate multiple repair and rehabilitation events involving multiple concrete mixes since the original 1910's construction.

Coarse aggregates used in most of the cores are either: (1) crushed limestone-dolomite (e.g., in Cores C-1a, 1b, 2b, 3a, 3b, 3d, 4a, 5a, 5b, and 7a), or, (2) crushed gravel (e.g., in Cores C-2a, 2c, 3c, 6a, 6b) where crushed limestone/dolomite used in the former series of cores are compositionally similar to each other indicating their derivation from the same or similar source, and, also crushed gravel in the second series of cores are also compositionally similar to each other, again indicting their derivation from similar source. Core C-4b has crushed granite, which is different from the other ones.

Despite compositional similarities of crushed limestone-dolomite, however, grain size, shape, and distribution of crushed limestone as well as the proportions of crushed stone to the mortar fractions of concrete varied considerably between the cores of the first series, indicating different crushing operations, which have provided a strong influence on the properties and performance of these concretes (since aggregates constitute 65 to 75 percent by volume of these cores).

For example for concrete in Core C-2b, crushed limestone/dolomite particles are mostly elongated, well-graded, and well-distributed where abundance of elongated particles has not only increased the water requirement of concrete but also created difficulty in effective filling of all interstitial spaces with the mortar fraction thereby leaving many coarse irregular-shaped entrapped voids between the particles resulting in weak aggregate-mortar bonds due to inadequate consolidation and filling of particles with mortar fraction to the extent of creating a 'dry pack' appearance of concrete. This has direct influence on the compressive strength, i.e., showing only 1590 psi strength.

For concrete in Core C-3b, crushed limestone/dolomite coarse aggregate particles are not elongated as seen in C-2b, mostly equidimensional with only a few elongated, but are poorly graded due to the deficiency of many finer and intermediate-size particles, which has increased the mortar fraction of concrete considerably. Unlike concrete in Core C-2b, interstitial spaces between the crushed stone particles are effectively filled with mortar fraction without any very coarse voids. The mortar fraction itself, however, showed many coarse entrapped voids though not as coarse or abundant as the voids seen in Core C-2b, and has soft, porous, high water-cement ratio paste. High mortar fraction of poor quality mortar due to poor grading of crushed stone aggregates has affected the compressive strength, with only 1900 psi strength reported for Core C-3b.

Fine aggregate in all cores are compositionally similar natural siliceous-argillaceous sand indicating derivation from similar source.

Pastes are Portland cement based at least in two cores examined by petrography, i.e., in Cores C-2b and 3b with no evidence of any pozzolanic or cementitious materials. Water-cement ratios varied considerably between the cores, e.g., from 0.45 to 0.50 in the paste in Core C-2b to 0.55-0.60 in the paste from Core C-3b.

Concretes in four cores examined by petrography (Cores C-2b and 3b) and air-void analysis (C-4b, and 6b) are all non-air-entrained with no indication of addition of any air entraining chemical. This is not surprising, especially if all these examined cores are representative of pre-1930's construction before air entrainment was discovered.

Perhaps the most startling evidence of variations in compositions, qualities, and conditions of concrete came from the large variations in compressive strength results provided, e.g., from as low as 1540 psi to as high as 6100 psi, where only one (1) out of 17 cores tested showed compressive strength above 6000 psi, three (3) others (except the > 6000 psi core) showed strength above 4000 psi, whereas the majority of 13 other cores showed strengths around 2000 psi even after almost 100 years of Portland cement hydration. Such overall low compressive strengths of majority of the cores indicate overall poor quality of concrete in terms of their low compressive strengths.

Nevertheless, since no major distress is reported at the locations of these cores, which is reasonably assumed to be due to their location in a protected or covered environment of train shed away from the typical harsh weather conditions of New York, i.e., from exposures to moisture, cyclic freezing and thawing, and chloride containing deicing chemicals, low strengths may not have affected their long-term durability. Based on the overall poor quality of concretes found, this study indicates the need to keep the concrete protected from the environment specially after finding their lack of air entrainment to degrade freeze-thaw durability and lack of adequate industry-recommended compressive strength of at least 4500 psi in the moist outdoor environment to affect both durability and long-term performance. Intermittent exposure to moisture and salt from trains passing by can bring some distress due to low strength and lack of air unless the concrete remains undersaturated during its service to prevent any freezing-related stress to develop. Abundant entrapped air despite lack of entrained air may in fact provide some benefit in providing rooms to accommodate frozen water and prevent freezing-related cracking or spalling.

All cores showed evidence of detectable but negligible water-soluble chloride and sulfate at the 3 in. and interior depths, which are indicative of lack of any chloride or sulfate exposure from the environment, which is consistent with the reported mild enclosed environment. Core C-3c showed the highest chloride content of all, though still not excessively higher than the common industry-recommended threshold chloride limit of 0.20 percent chloride by mass of cement for chloride-induced corrosion of steel in concrete to occur in the presence of oxygen and moisture. Sulfate contents are all within the values anticipated for contributions only from the Portland cement paste except the fact that the sulfate results are noticeably lower than the values for a concrete containing 15 percent Portland cement by mass (in which case sulfate content should have been 0.45 percent by mass of concrete containing 15 percent Portland cement where cement has sulfate content of 3 percent by mass), indicating use of lower-then-normal cement content in the cores, which is also indicative of the low compressive strength results reported.

INTRODUCTION

Reported herein are the results of detailed laboratory studies of seven hardened concrete cores reportedly collected from a train shed located below Park Avenue between 53rd and 55th Street in the Grand Central Terminal, Sector 2 in New York, New York.

BACKGROUND INFORMATION

Original concrete construction is reported to be circa 1910 - 1920 with miscellaneous repairs and rehabilitation projects since then. The concrete to be tested was reportedly not exposed to an outdoor environment of moisture, cyclic freezing and thawing or deicing chemicals since the samples came from inside a train shed in the enclosed structure below Park Avenue. Some locations, however, may have been exposed to roadway salts, but are reported to be still in a mild exposure condition. All samples were collected from the walls between train tracks in the train shed.

PURPOSE OF PRESENT INVESTIGATION

Based on the background information provided, the purposes of the present investigation are to determine:

a. The compositions, qualities, and overall conditions of concretes in the selected portions of two cores (Core No. C-2b and 3b) by detailed petrographic examinations;
b. Evidence of any physical or chemical deterioration of concrete in the selected portions of two cores (Core No. C-2b and 3b) by detailed petrographic examinations;
c. Air-void analyses of concretes in two cores (Core No. C-4b and 6b) to determine any potential role of air entrainment or lack thereof, on the short and long-term durability of concrete;
d. Water-soluble chloride, sulfate and other anion concentrations at 3 in. and interior (12 to 14.5 in.) depths to determine the depth of penetration of these ions during service; and
e. Evaluate results of compressive strength tests of all cores, which was done by another laboratory, in terms of the observed compositions of concrete in the present study.

SAMPLES

PHOTOGRAPHS, IDENTIFICATION, INTEGRITY, AND DIMENSIONS

Figures 1 through 17 show the detailed core photos, end surfaces of cores, visible cracks or voids, reinforcing steel, etc., along with testing done on each core.

Sample ID, Location	Length/ Diameter	End Surfaces	Cracks/Joints/ Large Voids	Reinforcing Steel	Integrity	Testing Done
C-1b Crash Wall	Length = 4 in. (100 mm) Diameter = 4 in. (100 mm)	Top - Dark Gray finished Bottom - Fresh Fractured	No visible cracks, joints, or coarse voids	None	Came in two saw-cut portions, each is intact (Figure 2)	Compressive Strength, Chloride at 3 in. and 12.5 in. depths
C-2b Column Encasement	Length = $3^{5}/_{8}$ in. (93 mm) Diameter = 4 in. (100 mm)	Top - Dark Gray finished Bottom - Fresh Fractured	No visible cracks, joints, but abundant coarse voids	No. 5 at $2^{3}/_{4}$ in depth	Came in two saw-cut portions, each is intact (Figure 4)	Compressive Strength, Petrography and Chloride at 3 in. and 13.75 in. depths
C-3b Crash Wall	Length = 7 in. (175 mm) Diameter = 4 in. (100 mm)	Top - Dark Gray finished Bottom – Saw-cut	No visible cracks, joints, or coarse voids	None	Came in one saw-cut portion which is intact (Figure 7)	Compressive Strength, Petrography
C-3c A-frame Encasement	Length = $6^{3}/_{4}$ in. (170 mm) Diameter = 4 in. (100 mm)	Top & Bottom – Sulfur capped from prior compressive strength testing	Extensive cracking throughout the depth due to prior compression testing	None	Came in one saw cut portion, which was strength-tested hence cracked (Figure 9)	Compressive Strength, Chloride at 3 in. and 7 in. depths
C-3d Crash Wall	Length = 4 in. (100 mm) + $4^{1}/_{2}$ in. (110 mm) Diameter = 4 in. (100 mm)	Top – Finished Bottom - Fresh Fractured	No visible cracks, joints, or coarse voids	None	Came in two saw-cut portions, each is intact (Figure 10)	Compressive Strength, Chloride at 3 in. and 14.5 in. depths
C-4b Crash Wall	Length = $6^{1}/_{4}$ in. (160 mm) Diameter = 4 in. (100 mm)	Top – Saw-cut Bottom - Fresh Fractured	No visible cracks, joints, or coarse voids	None	Came in one saw-cut portion, which is intact (Figure 12)	Compressive Strength, Air-Void Analysis
C-6b Crash Wall	Length = $7^{1}/_{2}$ in. (190 mm) + $5^{1}/_{2}$ in. (140 mm) Diameter = 4 in. (100 mm)	Top – Dark Gray finished Bottom – Sulfur Capped	Extensive cracking in one portion from strength testing, the other one is intact	None	Came in two saw-cut portions, one is intact the other strength tested hence cracked (Figure 15)	Compressive Strength, Air-Void Analysis, Chloride at 3 in. and 13.75 in. depths

Table 1: Dimensions, end surfaces, and conditions of only the portions of concrete cores, as received for this study. Compressive strength tests were not done by our laboratory.

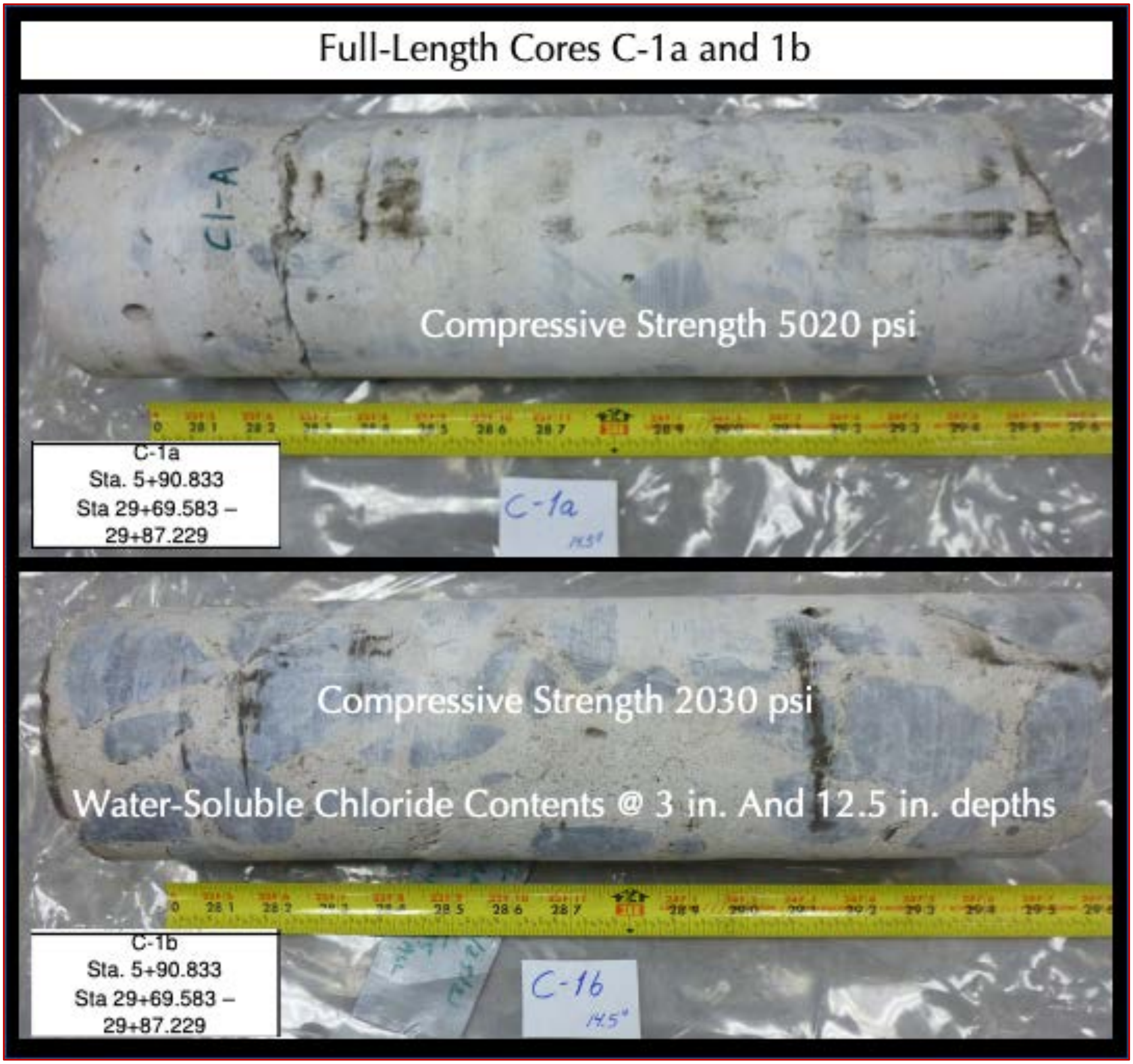

Figure 1: Full lengths of Cores C-1a and 1b, type of testing done, and compressive strength results.

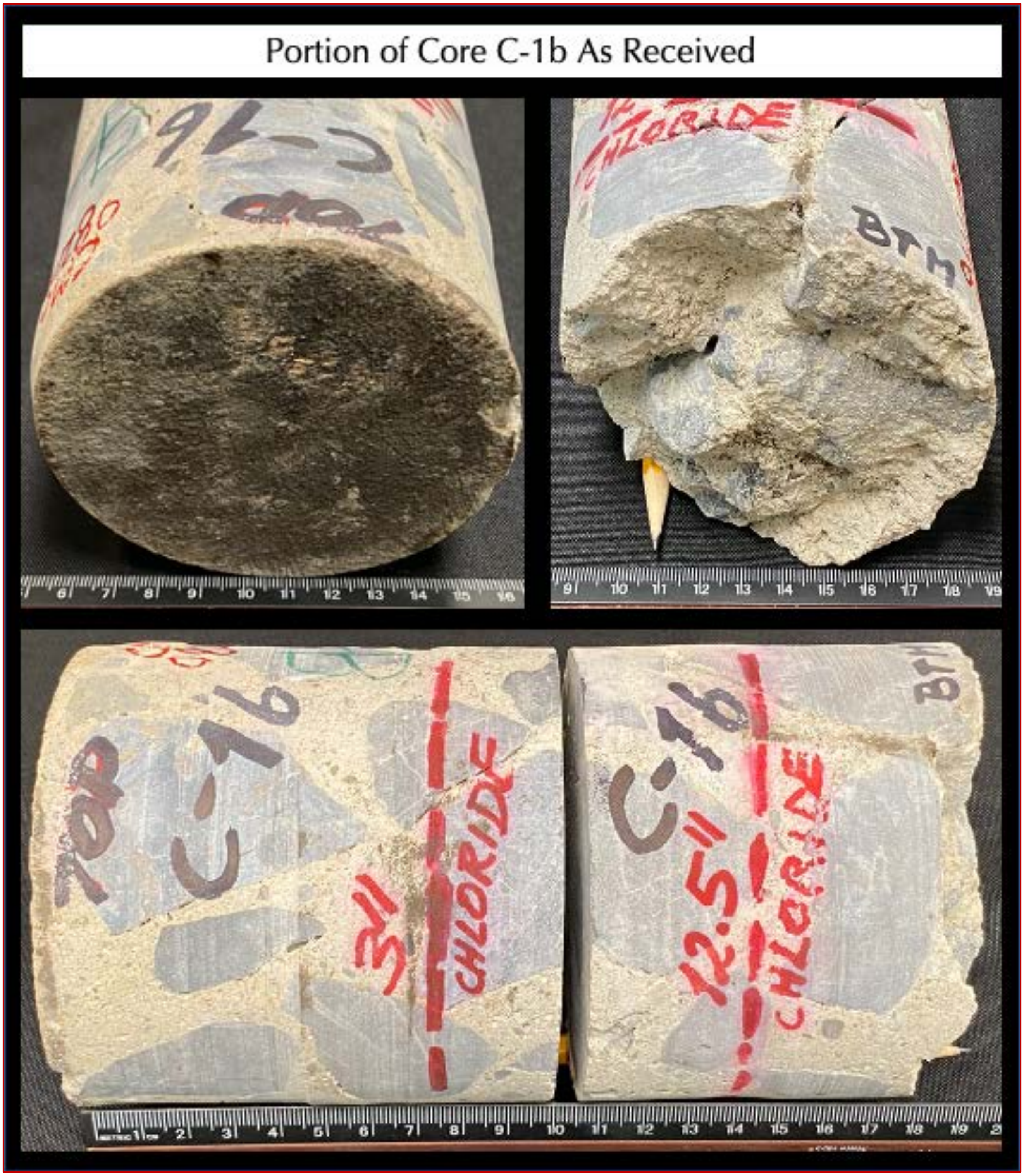

Figure 2: Portions of core as received from C-1b and the requested testing.

Figure 3: Full lengths of Cores C-2a and 2b, type of testing done, and compressive strength results.

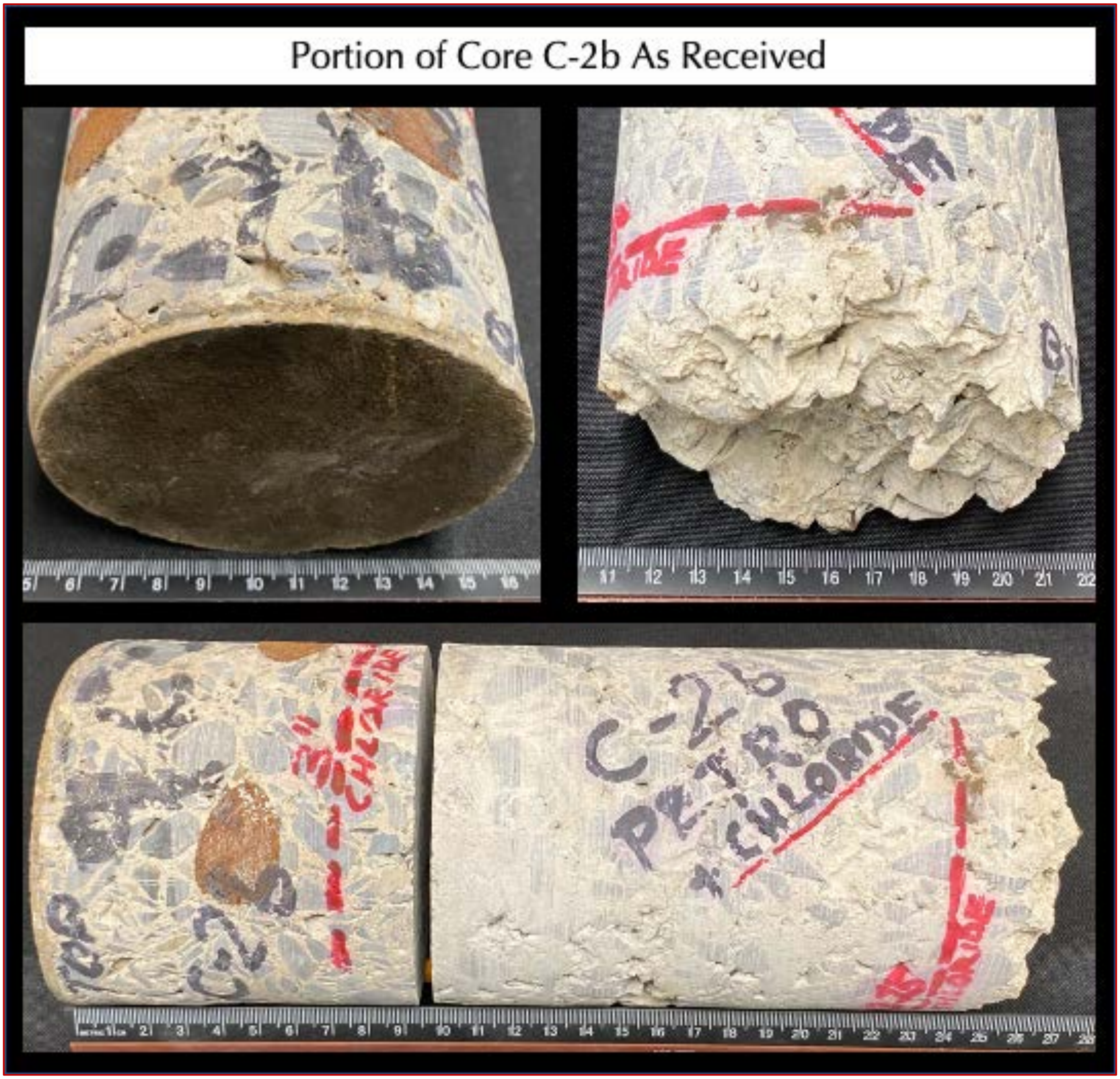

Figure 4: Portions of core as received from C-2b and the requested testing.

Figure 5: Full lengths of Cores C-2c and 2d, type of testing done, and compressive strength results.

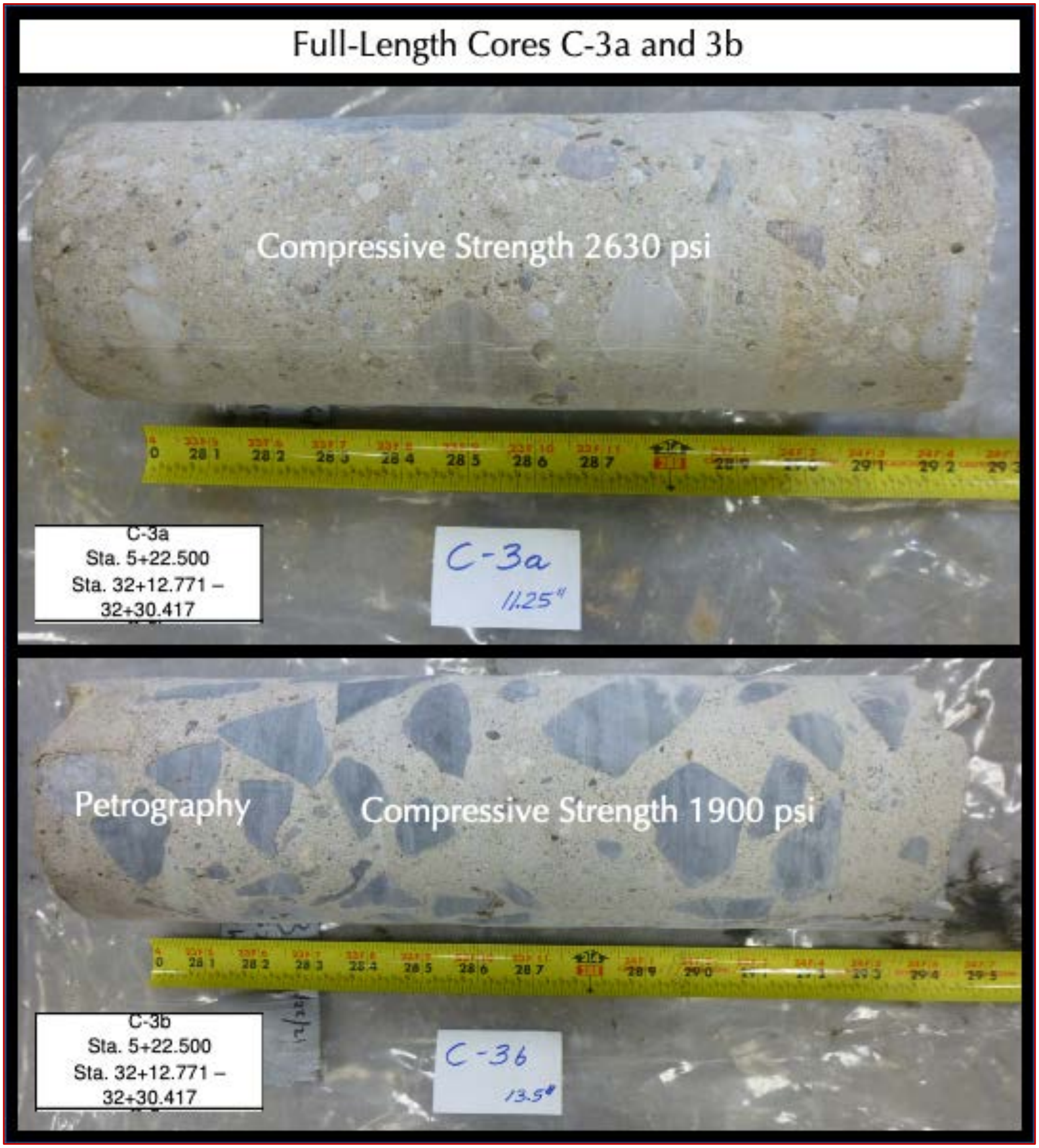

Figure 6: Full lengths of Cores C-3a and 3b, type of testing done, and compressive strength results.

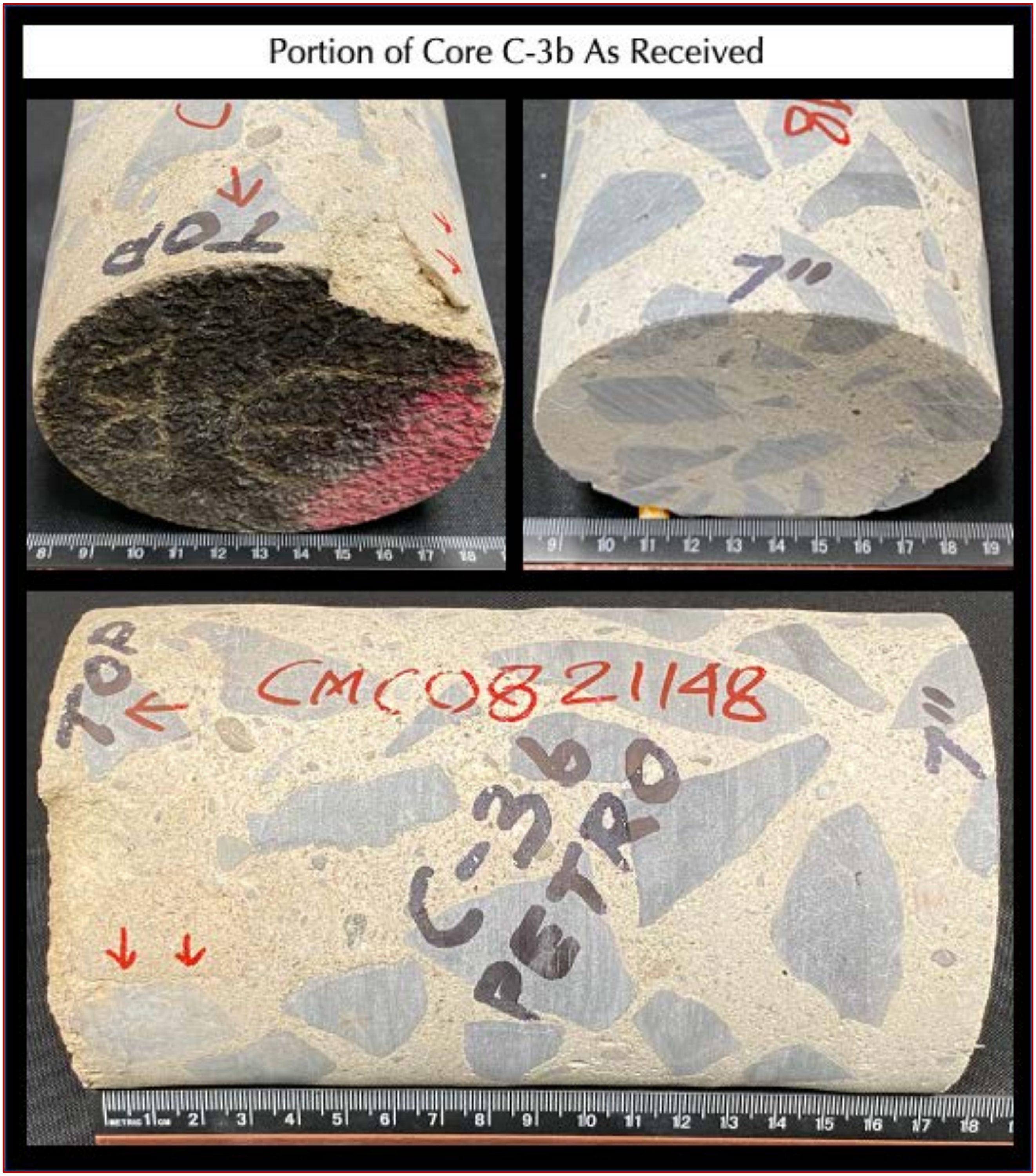

Figure 7: Portion of core as received from C-3b and the requested testing.

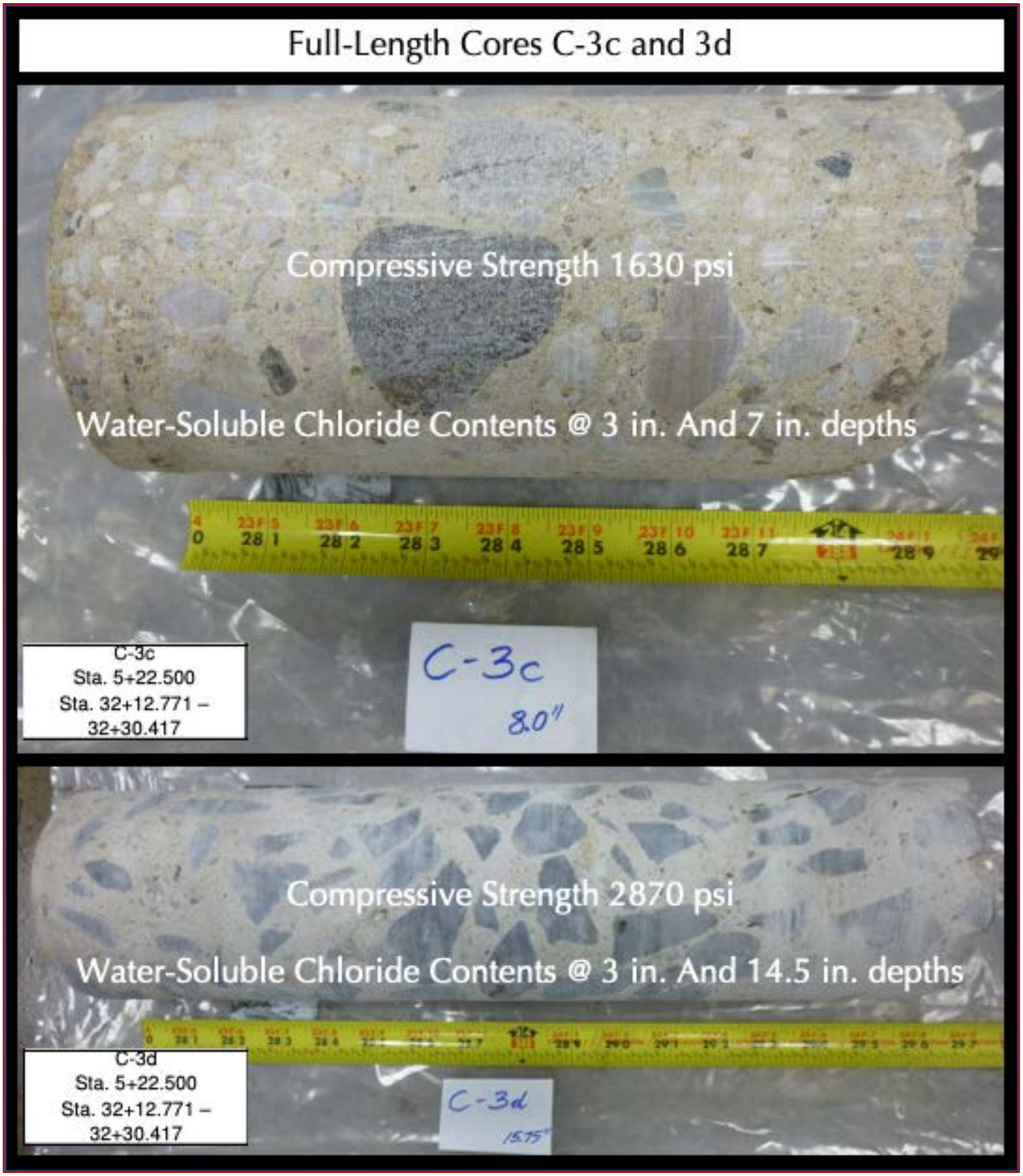

Figure 8: Full lengths of Cores C-3c and 3d, type of testing done, and compressive strength results.

Figure 9: Portion of core as received from C-3c and the requested testing.

Figure 10: Portions of core as received from C-3d and the requested testing.

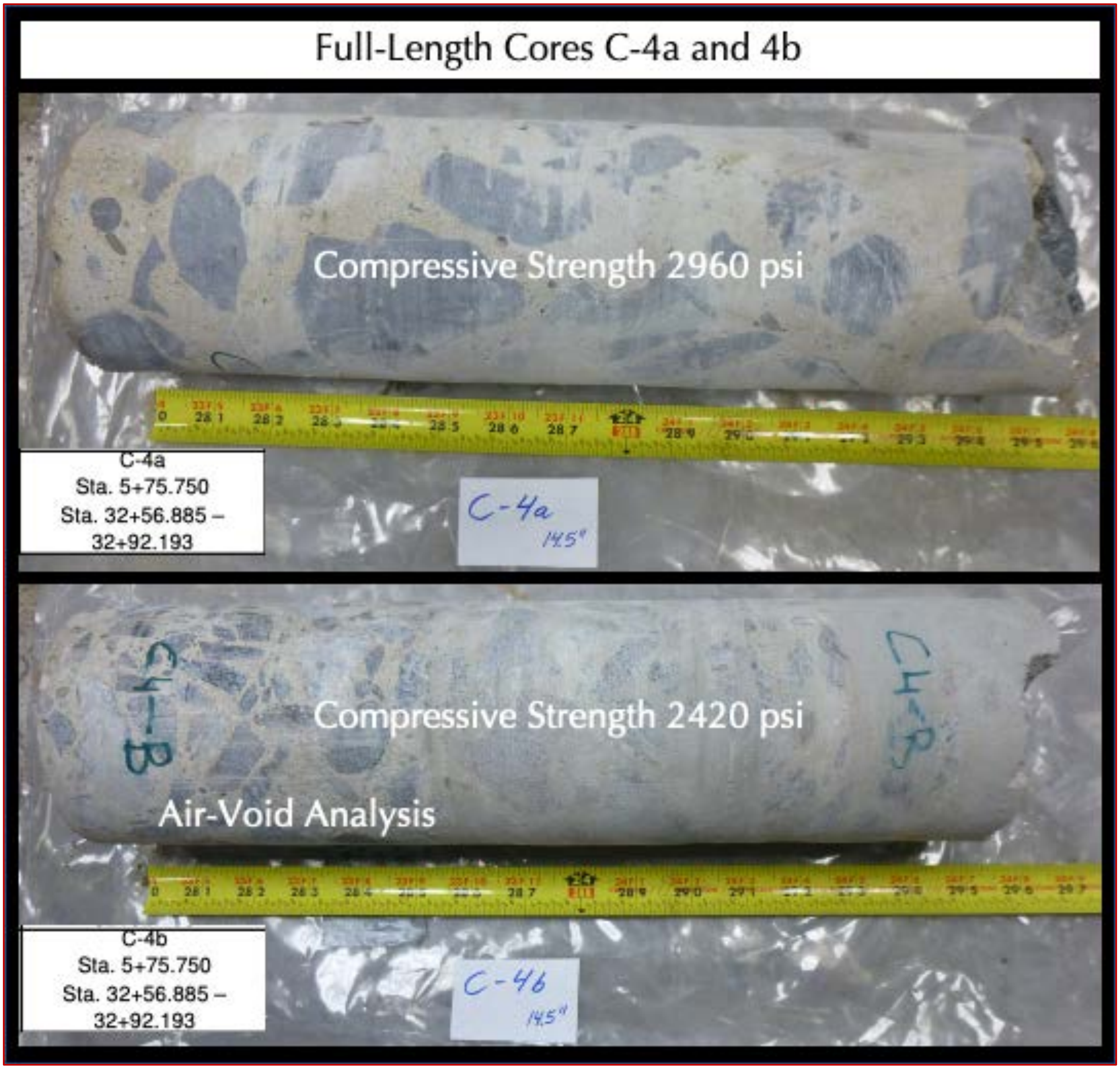

Figure 11: Full lengths of Cores C-4a and 4b, type of testing done, and compressive strength results.

Figure 12: Portion of core as received from C-4b and the requested testing.

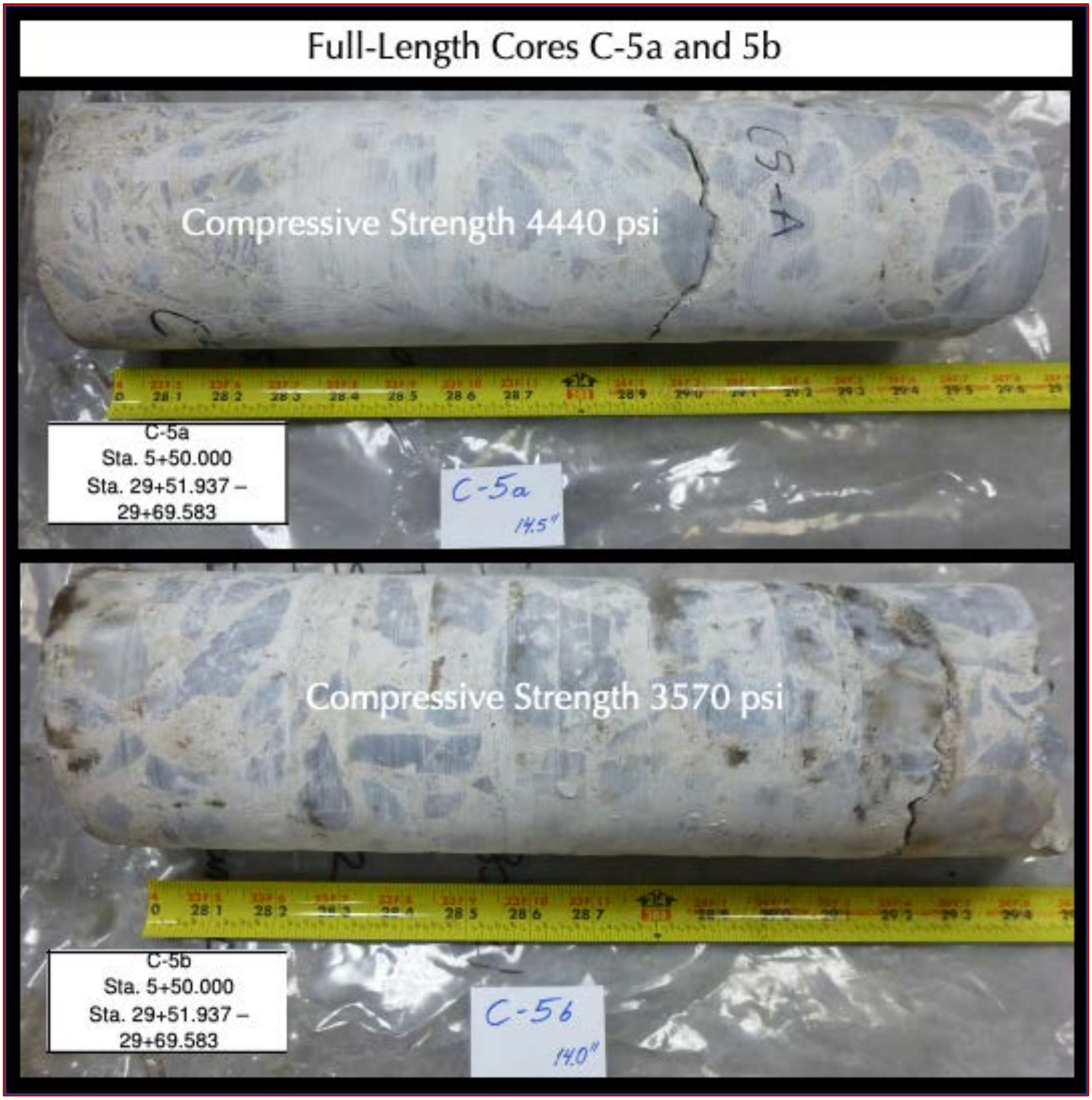

Figure 13: Full lengths of Cores C-5a and 5b, type of testing done, and compressive strength results.

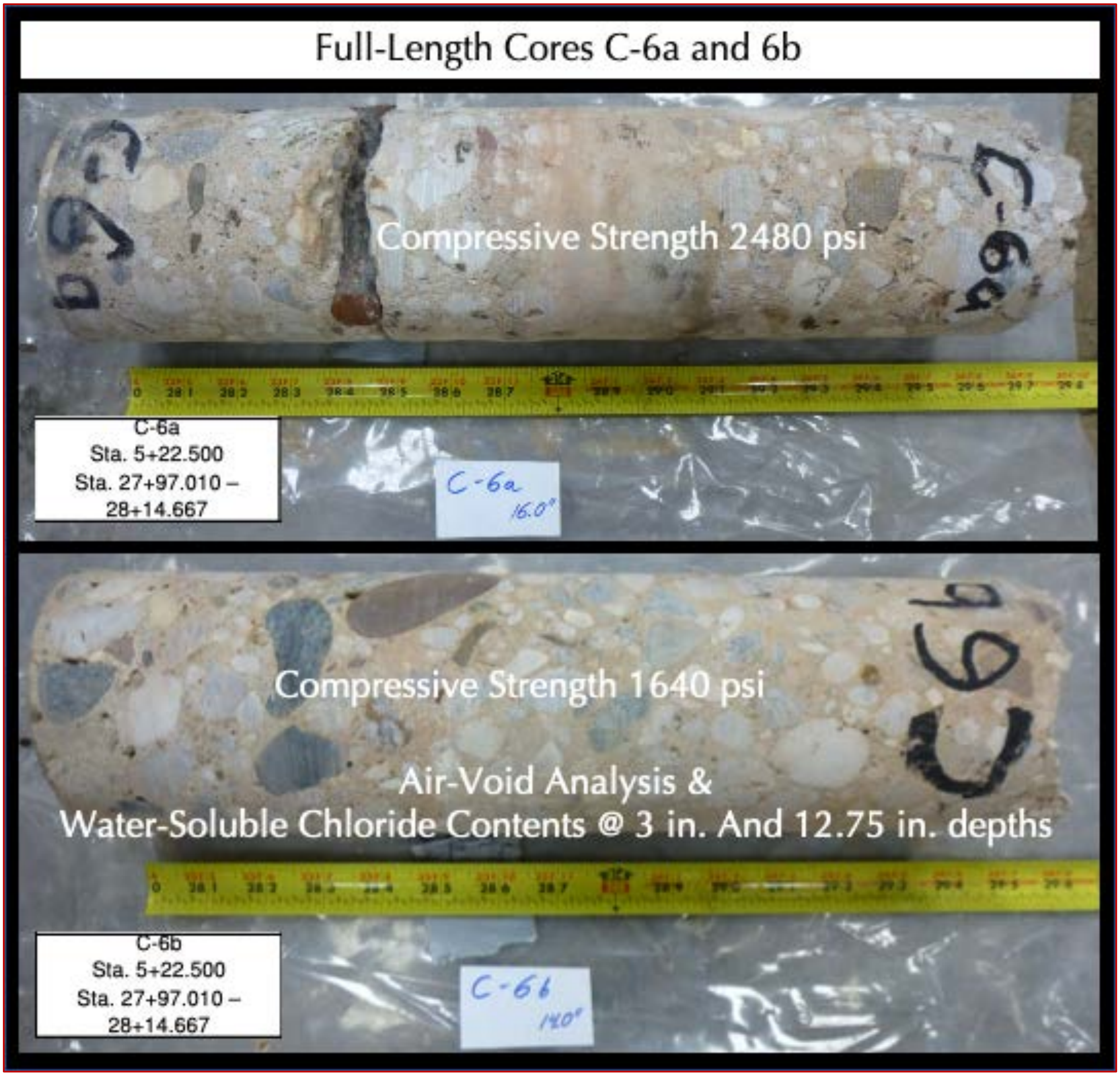

Figure 14: Full lengths of Cores C-6a and 6b, type of testing done, and compressive strength results.

Figure 15: Portions of core as received from C-6b and the requested testing.

Figure 16: Full lengths of Core C-7a, and compressive strength result.

Figure 17: Portions of cores received for petrographic examinations (Cores C-2b and 3b), air-void analysis (Cores C-4b and 6b), and depth markings for water-soluble chloride contents at two depths (Cores C-1b, 2b, 3c, 3d, and 6b).

METHODOLOGIES

PETROGRAPHIC EXAMINATIONS

Cores C-2b and C-3b were examined by detailed petrographic examinations according to the procedures of ASTM C 856 "Standard Practice for Petrographic Examination of Hardened Concrete." Details of petrographic examinations and sample preparation are described in Jana (1997a, b, 2004a, b, 2005a, b, 2006, 2007).

The steps of petrographic examinations include (Jana 2006):

i. Visual examinations of samples, as received;
ii. Low-power stereomicroscopical examinations of as-received, saw-cut and freshly fractured sections, and lapped cross sections of samples for evaluation of textures, and composition;
iii. Low-power stereomicroscopical examinations of air contents and air-void systems of concrete in the samples;
iv. Examinations of oil immersion mounts in a petrographic microscope for mineralogical compositions of specific areas of interest;
v. Examinations of blue dye-mixed (to highlight open spaces, cracks, etc.) epoxy-impregnated large area (50 mm × 75 mm) thin sections of concrete in a petrographic microscope for detailed compositional and microstructural analyses;
vi. Photographing samples, as received and at various stages of preparation with a digital camera and a flatbed scanner;
vii. Micrographs of lapped sections and thin sections of samples taken with stereomicroscope and petrographic microscope, respectively to provide detailed compositional and mineralogical information of concrete.

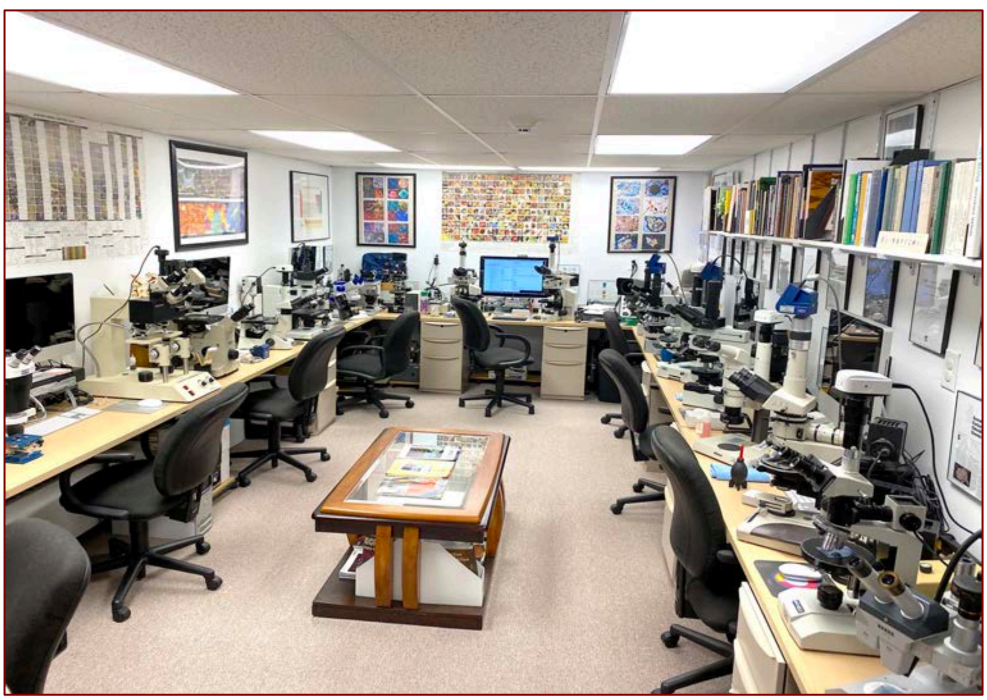

Figure 18: CMC's petrographic laboratory that houses various optical microscopes used in this study.

AIR-VOID ANALYSIS

Cores C-4b and C-6b were examined by using the ASTM Standard Practice of air-void analysis by following the modified point count method, as mentioned in ASTM C 457 "Standard Test Method for Microscopical Determination of Parameters of the Air-Void System in Hardened Concrete," where the steps followed during air-void analysis are given below.

a. The Velmex point-count device used in the analysis (see Figure 19) is comprised of a platform connected to E-W and N-S lead screws and designed in such a way that a lapped concrete sample placed on the stage can be moved smoothly and uniformly through equal distances by turning of the screws. It was ensured that the total possible translation of the stage was at least 100 mm (4.0 in.) in each direction. Lead screws were fitted with notched wheels and stopping devices, such that with each rotation of the screws the operator can detect a click when a stop position was reached. It was ensured that the intervals between the stops correspond to a translation of the stage a distance of 0.025 to 0.64 to 5.0 mm (0.025 to 0.200 in.). The magnitude of the average translation of the stage between stops was determined to the nearest 0.03 mm (0.001 in.). A total of six digital counters were used for calculating aggregates, paste, entrained and entrapped voids, and total voids intercepted during the traverse.

b. A high-resolution digital microscope camera attached to a research-grade high-resolution stereomicroscope was used to capture live images of the lapped concrete surfaces on the PC screen.

c. A lapped section of concrete was place on the stage of the point-count device. Using the spirit level, the prepared surface was leveled with the leveling device so that the surface may be traversed and microscopically examined with a minimum of refocusing. Lamp was adjusted so the beam evenly illuminated the field of view of the microscope and was incident upon the surface at a low angle, so the air voids were demarked by a shadow. Superimposed in the computer screen was the index point of the cross hairs to pinpoint the area to be counted. A magnification not less than 50X was used and wasn't changed during the course of the analysis. For a rectangular lapped section, the index was placed near an upper corner (for a circular section, it is usually placed near the top) and at one end of the initial traverse. The stopping device was positioned at a stop or click position at the beginning of the traverse. The initial stops for each traverse line were not included in the total number of stops or in the number of stops for any component. Zeroed all counters. By operation of the E-W lead screw, caused movement of the stage and specimen while simultaneously scrutinizing the surface. At each click stop, except not at the beginning of any traverse line, paused and examined the field of view, and recorded on the appropriate counter the material or phase on which the index point was superimposed. Normally used one counter for air voids, one for paste, and one for all other phases (or a totaling counter). Other components (fine and coarse aggregate, for example—if they are lithologically distinguishable) of the concrete was determined with the use of additional counters. Continued in this way along the line until a last stop is reached just within the prepared area, but close to its edge. When the end of the line is reached, turned off the totaling counter. Reversed the E-W lead screw and proceeded back along the same line, recording on another counter each air void intersected, whether or not a stop has occurred within the air void. Terminated the void counting just before the initial stop. Took extreme care to determine whether a section of an air void was intersected by the movement of the index when the line of traverse is nearly tangent to the void section. The results can be affected significantly by consistent error in this respect. If the periphery of an air void was crumbled or rounded, estimated the position of the true periphery in the plane of the surface by extrapolation of the surface contour of the air void. If the examination was being made to determine only the air content of the concrete, the number of air voids intersected by the line of traverse need not be determined. By means of the N-S lead screw, shifted the concrete specimen at right angles to the direction of traverse an appropriate distance. Spaced the segments of the traverse so as to cover the whole prepared surface and achieved at least the minimum length of traverse and the minimum number of points specified in C 457. Proceeded along the new line of traverse as before, and so on, for all segments of the total traverse and for all sections prepared from a sample of concrete so as to comply with the requirements of this test method.

d. Minimum length of traverse and minimum number of points for the modified point count method are: (a) 2540 mm (100 in.) and 1500 points for $1\frac{1}{2}$-in. nominal size aggregate, (b) 2413 mm (95 in.) and 1425 points for 1-in. nominal size aggregate, (c) 2286 mm (90 in.) and 1350 points for $\frac{3}{4}$-in. nominal size aggregate, (d) 2032 mm (80 in.) and 1200 points for $\frac{1}{2}$-in. nominal size aggregate, and (e) 1905 mm (75 in.) and 1125 points for $\frac{3}{8}$-in. nominal size aggregate.

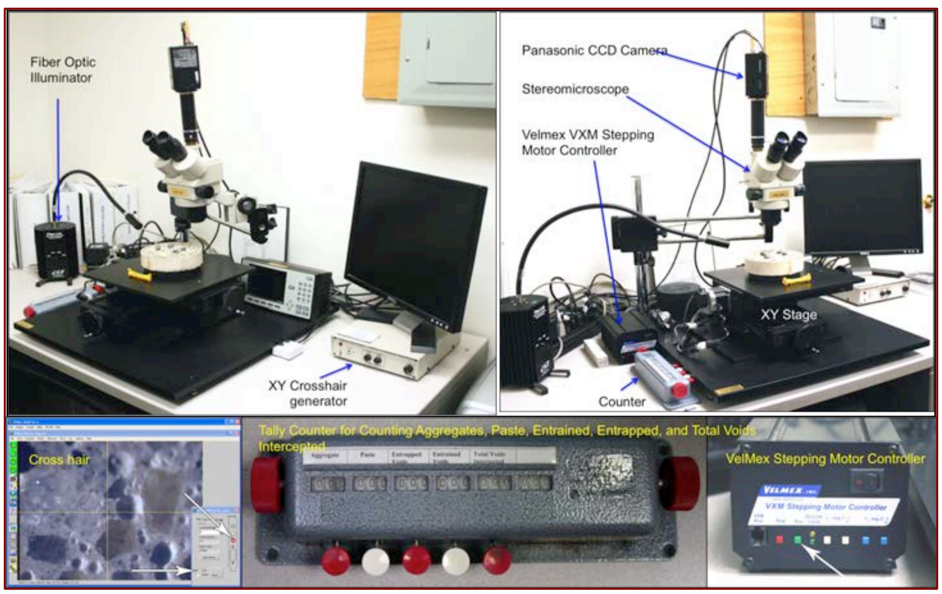

Figure 19: Set-up in the CMC laboratory for air-void analysis in hardened concrete by the modified point count method of ASTM C 457.

e. Air-void parameters were calculated by using the equations provided in C 457.

f. Two cores were sectioned vertically through depth (Figures 23 and 24) to examine through-depth variations of air contents.

CHEMICAL PROFILES OF CHLORIDE, SULFATE, AND OTHER WATER-SOLUBLE ANIONS

Portions of pulverized concrete sectioned from the marked locations at 3 in. depths and 12 through 14.5 in depths in the cores were digested in deionized water for 24 hours at room temperature, and then filtered to collect the filtrates for determination of various anions by ion chromatography by following the methods of ASTM D 4327, particularly for water-soluble chloride and sulfate ion contents in concrete.

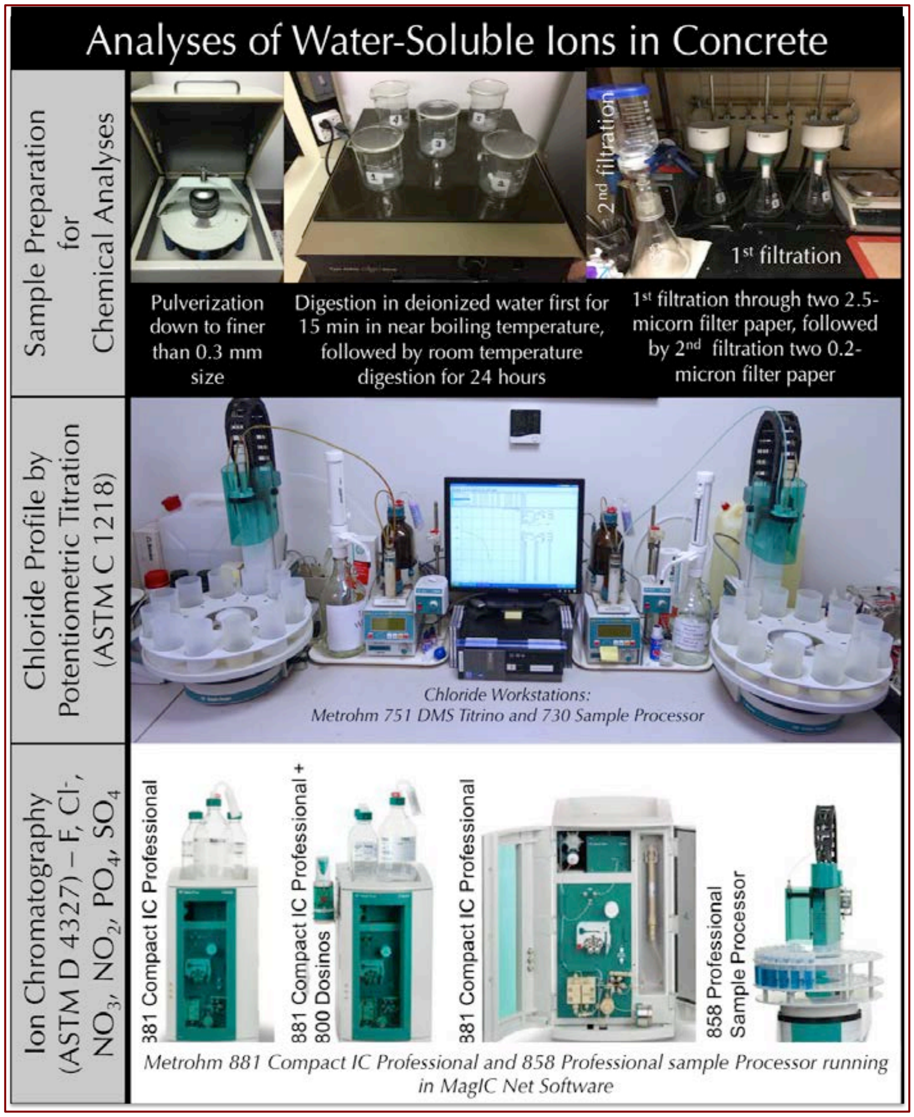

Figure 20: Sample preparation and analyses of water-soluble ions in concrete by potentiometric titration or ion chromatography.

Sections were pulverized down to finer than 0.3 mm size. Approximately 10 grams of pulverized concrete from each section was thoroughly digested in 100 ml deionized water first in near-boiling temperature for 15 minutes with magnetic stirrer, followed by further room-temperature digestion for 24 hours. The digested sample solution was then filtered under vacuum, first through two 2.5-micron filter papers, followed by another filtration through two 0.2-micron filter papers to collect the filtrate. The filtrate thus obtained was diluted to a final volume of 200 ml in a volumetric flask.

Filtrate thus prepared was used for anion chromatography, *a la* ASTM D 4327 for water-soluble fluoride, chloride, nitrate, nitrite, bromide, phosphate, and sulfate ions by using Metrohm 881 Compact IC Professional with attached 858 Professional Sample Processor with a sodium carbonate-bicarbonate eluent (Figure 20).

PETROGRAPHIC EXAMINATIONS

LAPPED CROSS SECTIONS

Figure 21: Lapped cross section of a middle portion of Core C-2b having a saw-cut end at one side and fractured end at the opposite side, showing:

(a) Crushed limestone-dolomite coarse aggregate where most particles are elongated, which usually increases water requirement of concrete, angular, well-graded, and well-distributed;

(b) Interstitial mortar fraction of siliceous-calcareous-argillaceous sand and Portland cement paste having a soft, porous, high water-cement ratio paste;

(c) Notice abundant coarse, irregularly-shaped entrapped voids left from inadequate filling of interstitial spaces between crushed stone coarse aggregate, that have provided a dry-pack appearance of concrete with the resultant very low (in fact the lowest) reported compressive strength of 1590 psi.

Figure 22: Lapped cross section of top portion of Core C-3b having weathered exposed end at one side and a saw-cut end at the opposite side, showing:

(a) Crushed limestone-dolomite coarse aggregate where most particles are very coarse in size, mostly equant to a few elongated, dense, poorly graded due to the deficiency of some finer and intermediate sizes of coarse aggregate, and poorly distributed with some segregation of particles beneath $^{1}/_{2}$ in. of exposed surface;

(b) Interstitial mortar fraction of siliceous sand and Portland cement paste having a soft, porous, high water-cement ratio paste; and,

(c) Reported compressive strength of concrete is 1900 psi, which is attributed mainly to the soft, porous, high water-cement ratio nature of the interstitial paste.

Figure 23: Lapped cross section of middle portion of Core C-4b having a saw-cut end at one side and a fresh fractured end at the opposite side, showing:

(a) Crushed stone coarse aggregate where most particles are equant to a few elongated, dense, well-graded and well-distributed;

(b) Interstitial mortar fraction of siliceous sand and Portland cement paste having a soft, porous, high water-cement ratio paste;

(c) Reported compressive strength of concrete is 2420 psi, which is attributed mainly to the soft, porous, high water-cement ratio nature of the interstitial paste.

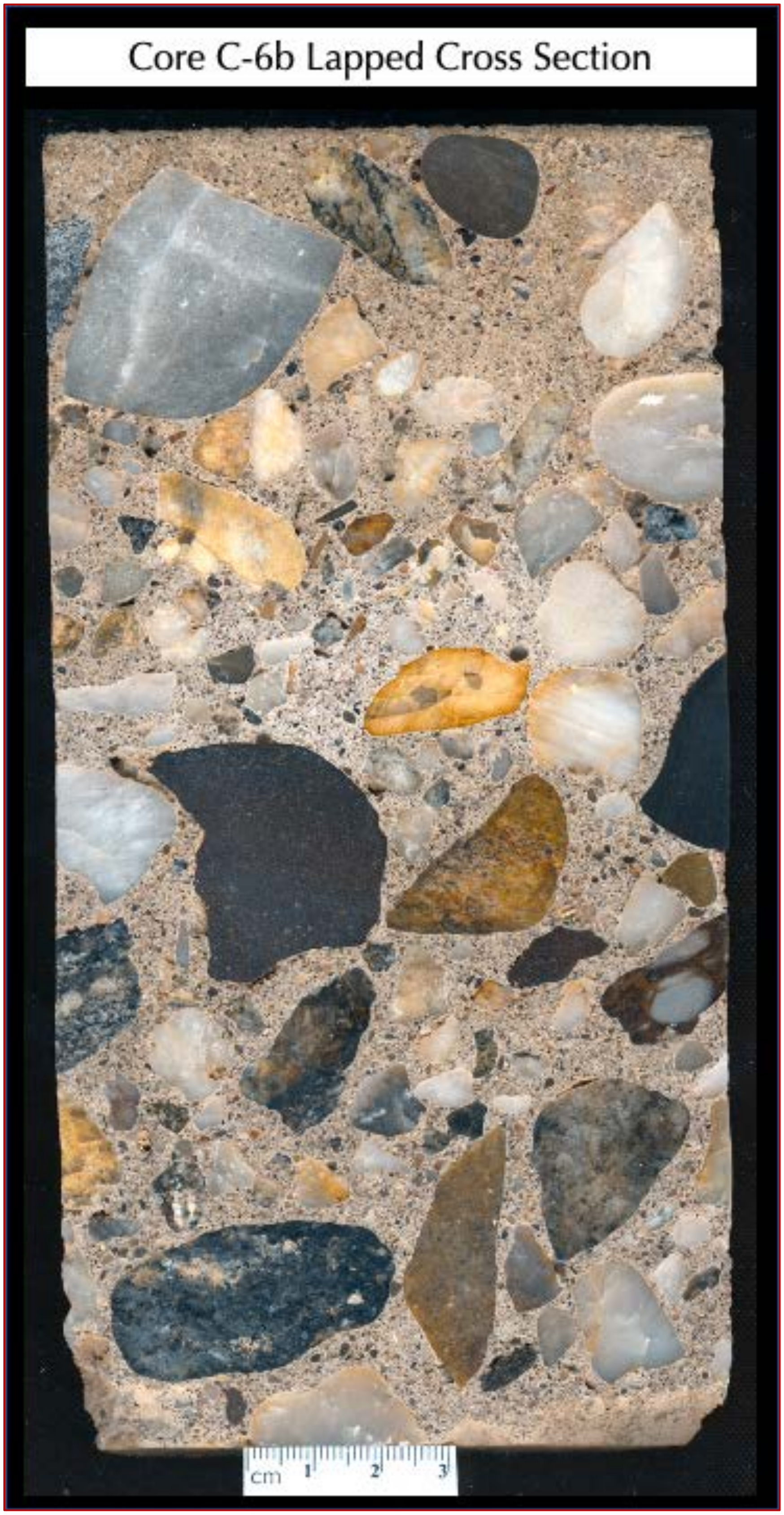

Figure 24: Lapped cross section of top portion of Core C-6b having a weathered exposed end at one side and a saw-cut end at the opposite side, showing:

(a) Lightly crushed gravel coarse aggregate where most particles are well-rounded to subrounded depending on crushing, mostly equant to a few elongated, dense, well-graded and well-distributed;

(b) Interstitial mortar fraction of siliceous sand and Portland cement paste having a soft, porous, high water-cement ratio paste; and,

(c) Reported compressive strength of concrete is 1640 psi, which is attributed mainly to the soft, porous, high water-cement ratio nature of the interstitial paste.

MICROGRAPHS OF LAPPED CROSS SECTIONS

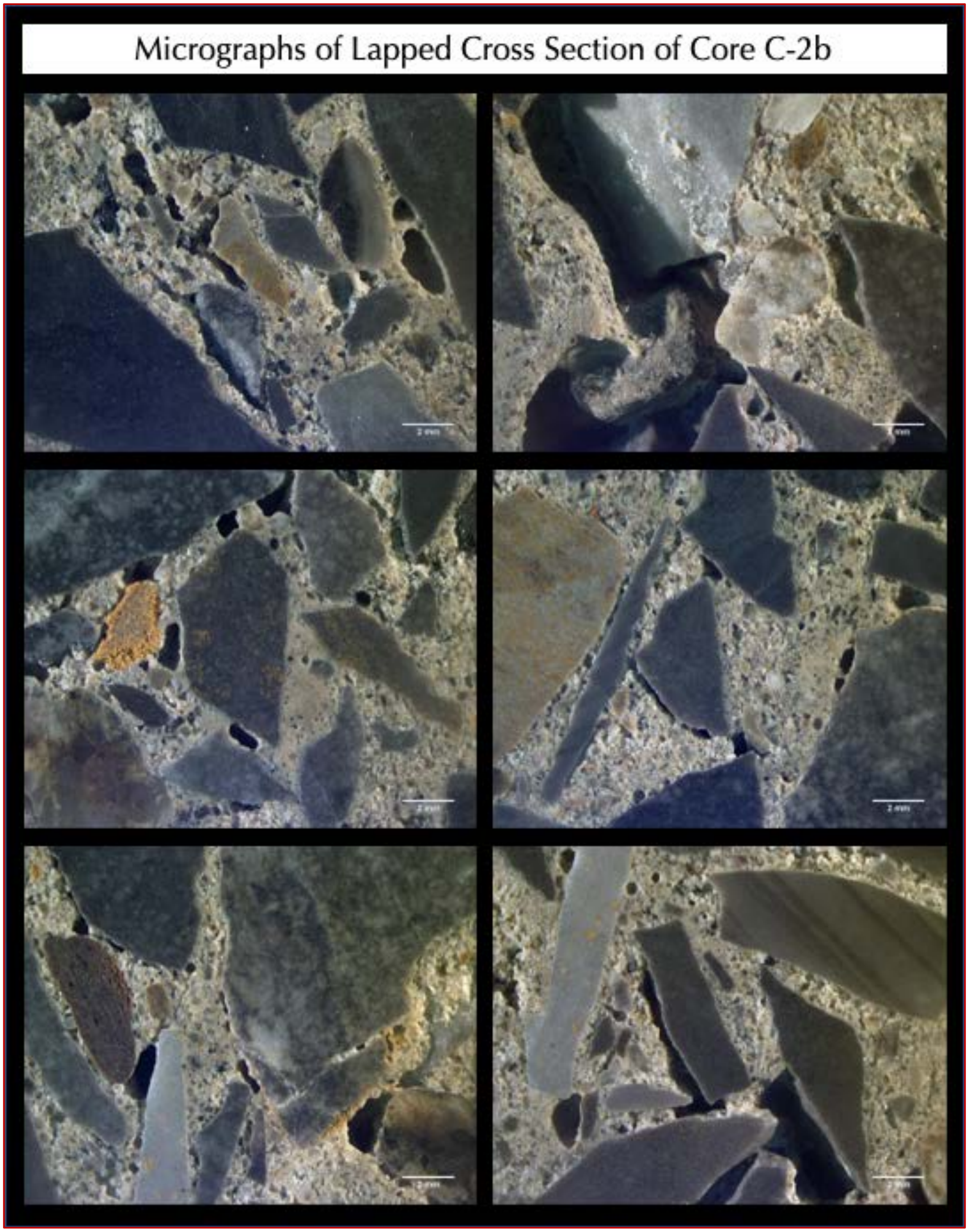

Figure 25: Micrographs of lapped cross section of Core C-2b showing: (a) abundant coarse, irregularly-shaped entrapped air voids due to inadequate consolidation of concrete leaving lots of interstitial spaces between crushed limestone-dolomite coarse aggregate particles thereby giving a dry-pack appearance of concrete, and (b) lack of air entrainment in the concrete despite abundant entrapped voids to lower the compressive strength to the lowest of the report ones.

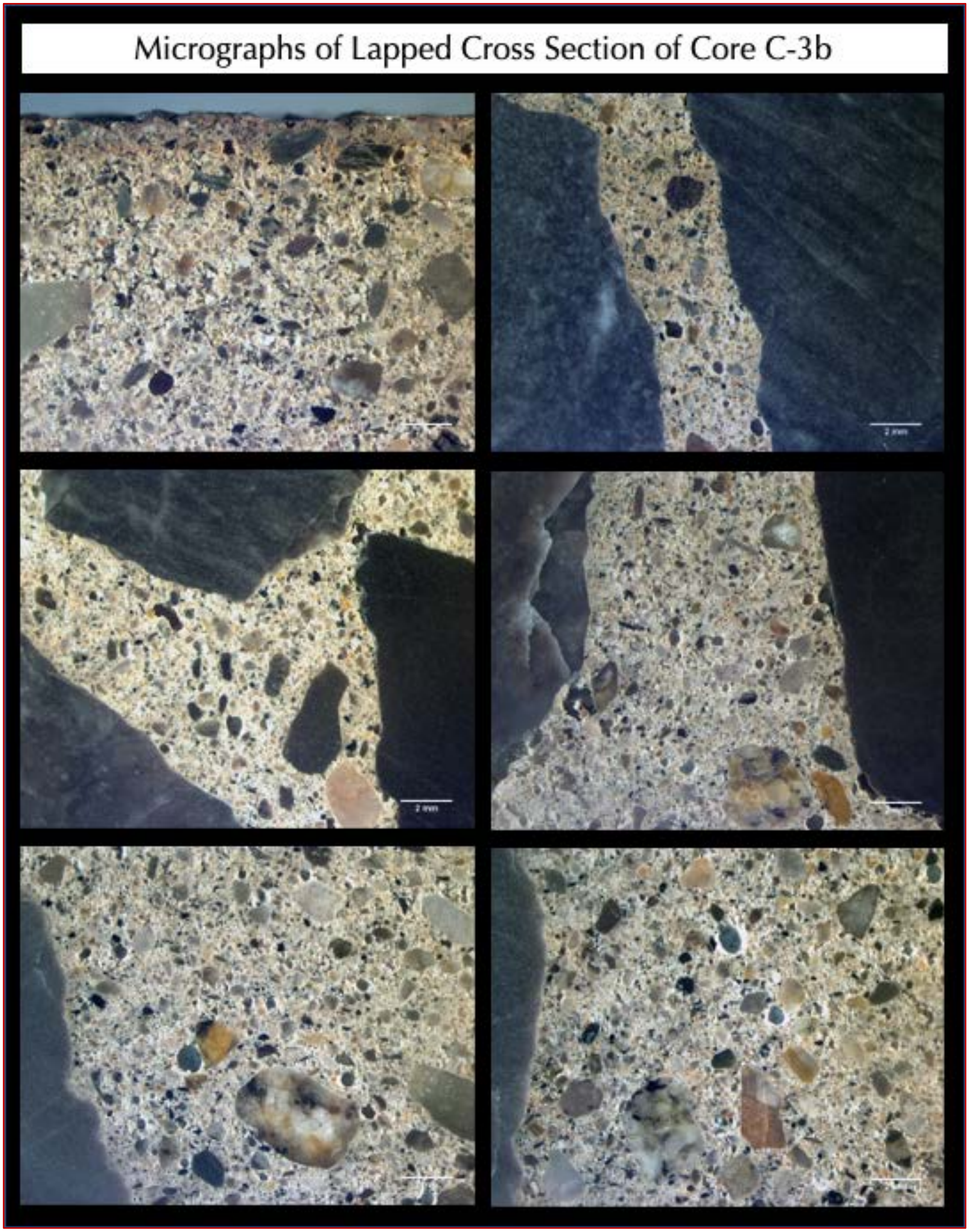

Figure 26: Micrographs of lapped cross section of Core C-3b showing: (a) the overall non-air-entrained nature of concrete having a few discrete, spherical and near-spherical entrapped air bubbles, and (b) overall porous but well-consolidated nature of concrete.

Figure 27: Micrographs of lapped cross section of Core C-4b showing: (a) the overall non-air-entrained nature of concrete having a few discrete, spherical and near-spherical entrapped air bubbles, and (b) overall porous but well-consolidated nature of concrete.

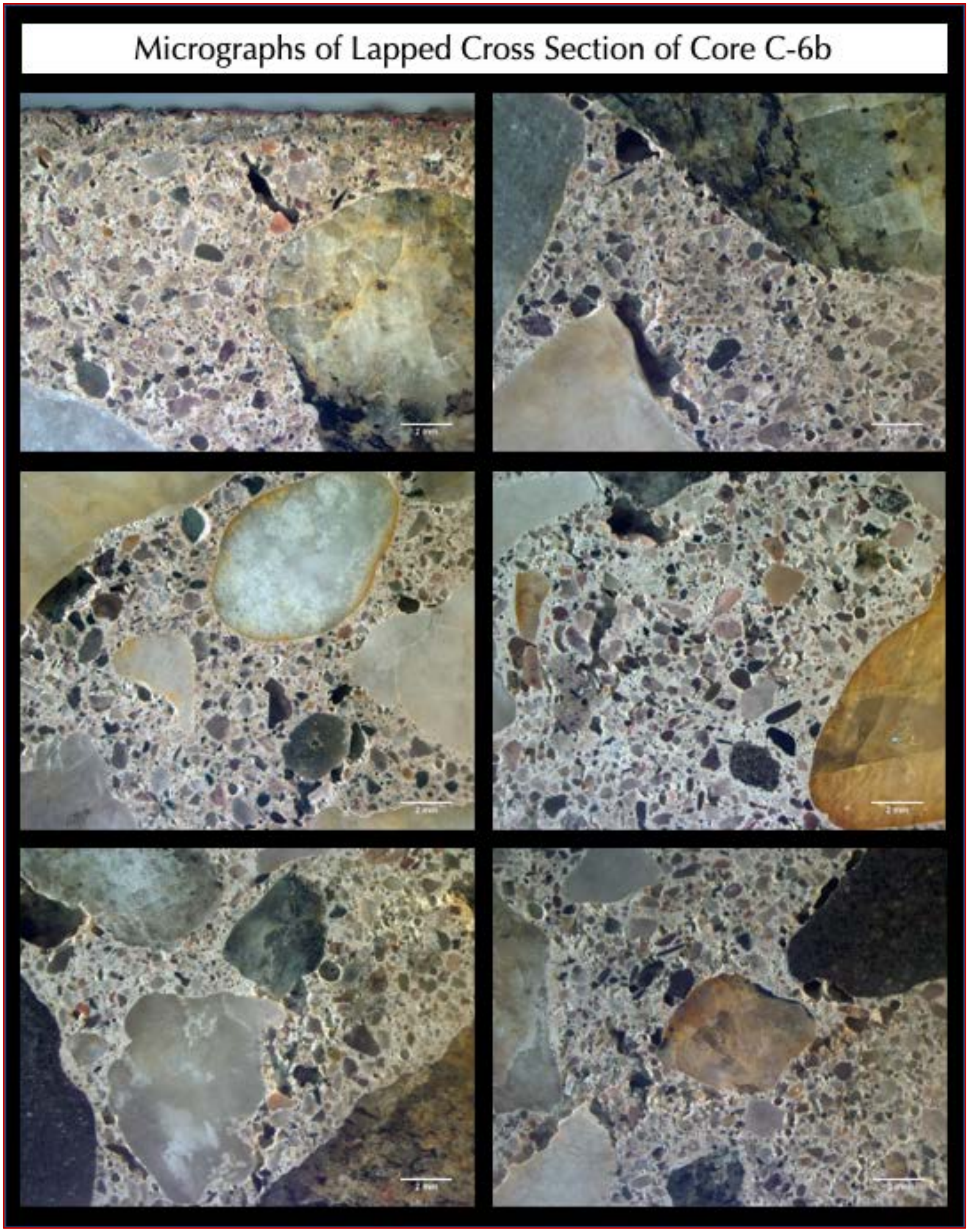

Figure 28: Micrographs of lapped cross section of Core C-6b showing: (a) the overall non-air-entrained nature of concrete having a few discrete, spherical and near-spherical entrapped air bubbles, and (b) overall porous but well-consolidated nature of concrete.

BLUE DYE-MIXED EPOXY-IMPREGNATED THIN SECTIONS

Figure 29: Enlarged view of a 50 mm × 75 mm size blue dye-mixed epoxy-impregnated thin section of Core C-2b, shown in plane polarized light mode by scanning the thin section on a flatbed scanner with a polarizing filter. The image highlights abundant coarse entrapped air voids in the concrete due to inadequate filling of interstitial spaces between elongated crushed limestone-dolomite coarse aggregate leaving only minor mortar fraction of natural siliceous-argillaceous sand fine aggregate and Portland cement paste.

Figure 30: Enlarged view of a 50 mm × 75 mm size blue dye-mixed epoxy-impregnated thin section of Core C-2b, shown in crossed polarized light mode by scanning the thin section on a flatbed scanner with two perpendicular polarizing filters between the thin section. The image highlights crushed limestone-dolomite coarse aggregate leaving only minor mortar fraction of natural siliceous-argillaceous sand fine aggregate and Portland cement paste.

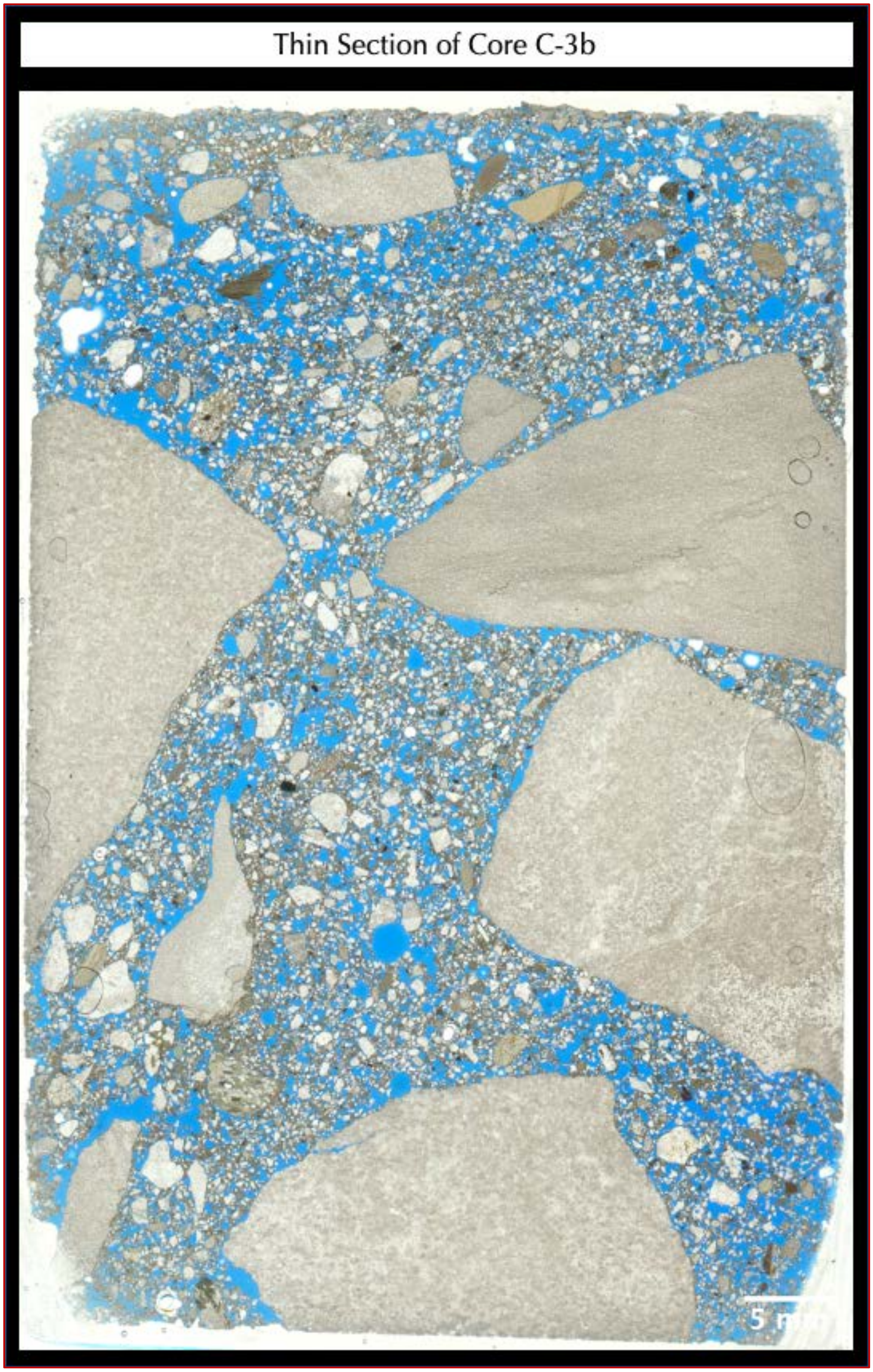

Figure 31: Enlarged view of a 50 mm × 75 mm size blue dye-mixed epoxy-impregnated thin section of Core C-3b, shown in plane polarized light mode by scanning the thin section on a flatbed scanner with a polarizing filter. The image highlights crushed limestone-dolomite coarse aggregate and an interstitial mortar fraction of natural siliceous-argillaceous sand fine aggregate and Portland cement paste. Concrete is non air-entrained but contains many coarse entrapped air voids in the mortar fraction, which is responsible for reported low compressive strength of 1900 psi.

Figure 32: Enlarged view of a 50 mm × 75 mm size blue dye-mixed epoxy-impregnated thin section of Core C-3b, shown in cross polarized light mode by scanning the thin section on a flatbed scanner with two perpendicular polarizing filters between the thin section. The image highlights crushed limestone-dolomite coarse aggregate and an interstitial mortar fraction of natural siliceous-argillaceous sand fine aggregate and Portland cement paste.

MICROGRAPHS OF THIN SECTIONS

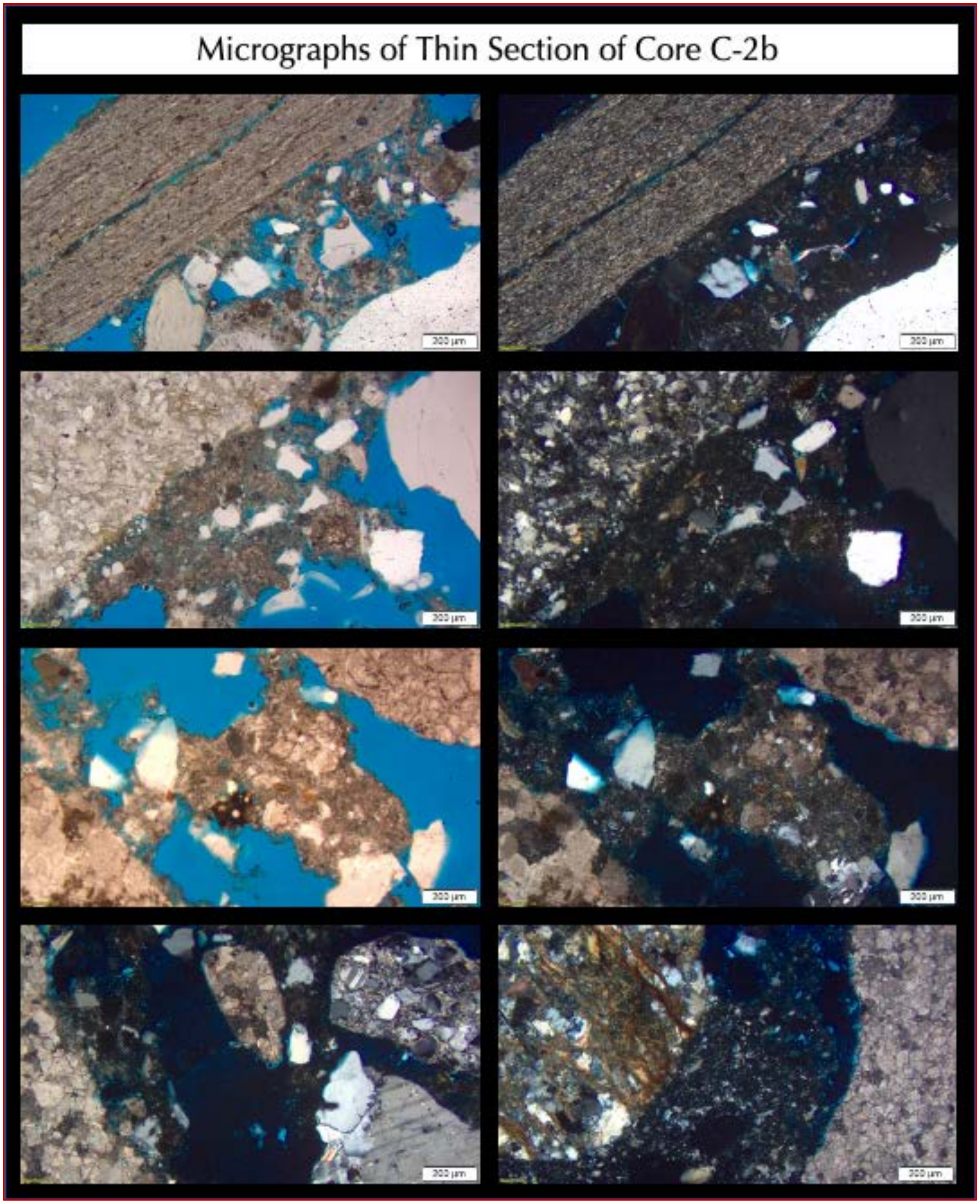

Figure 33: Micrographs of thin section of Core C-2b showing crushed limestone-dolomite coarse aggregate, natural siliceous (quartz, quartzite, quartz siltstone and sandstone), calcareous (limestone, dolomite), and argillaceous (shale) sand particles in fine aggregate, and Portland cement paste that has inadequately coated the aggregates.

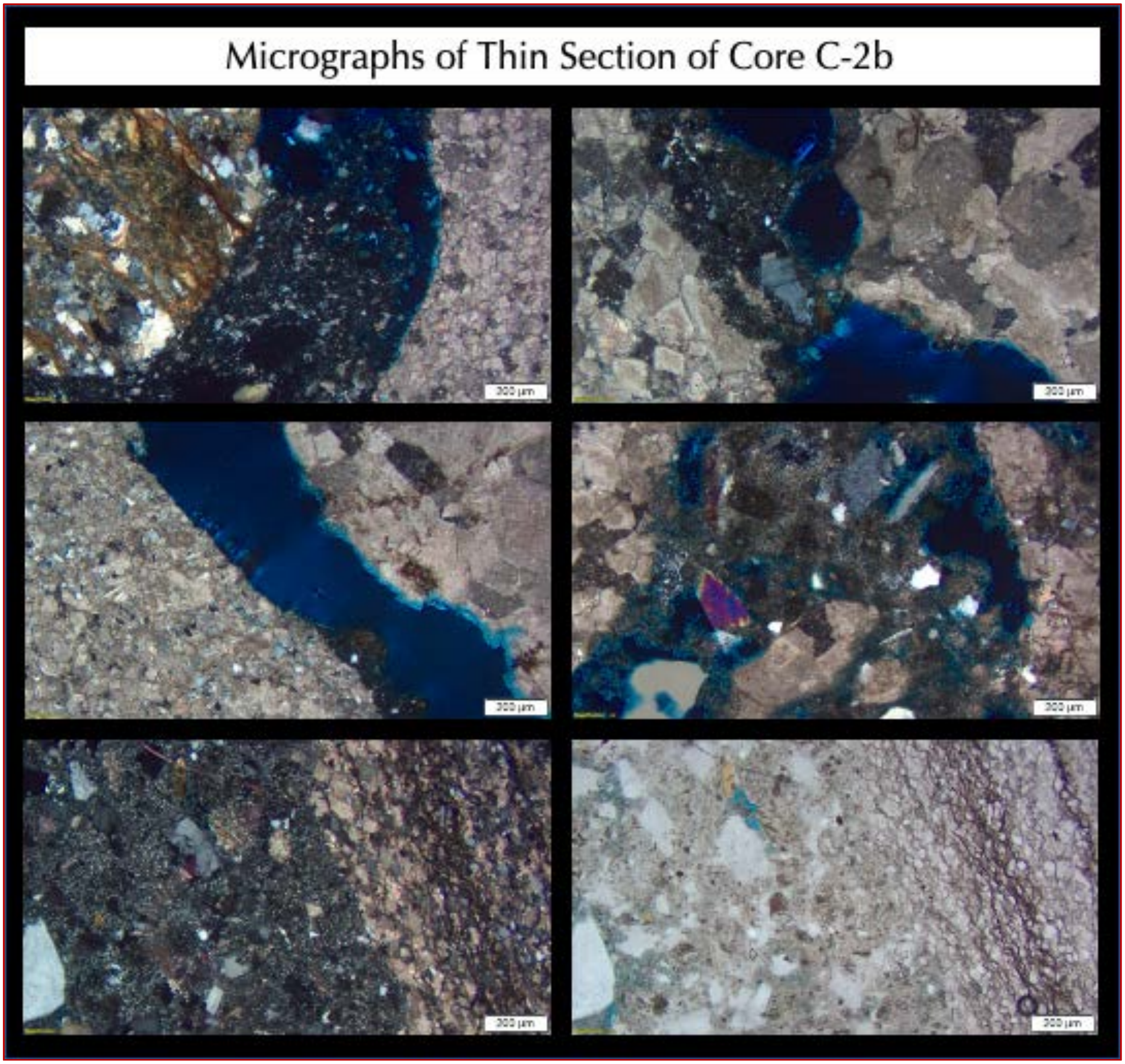

Figure 34: Micrographs of thin section of Core C-2b showing crushed limestone-dolomite coarse aggregate, natural siliceous (quartz, quartzite, quartz siltstone and sandstone), calcareous (limestone, dolomite), and argillaceous (shale) sand particles in fine aggregate, and Portland cement paste that has inadequately coated the aggregates.

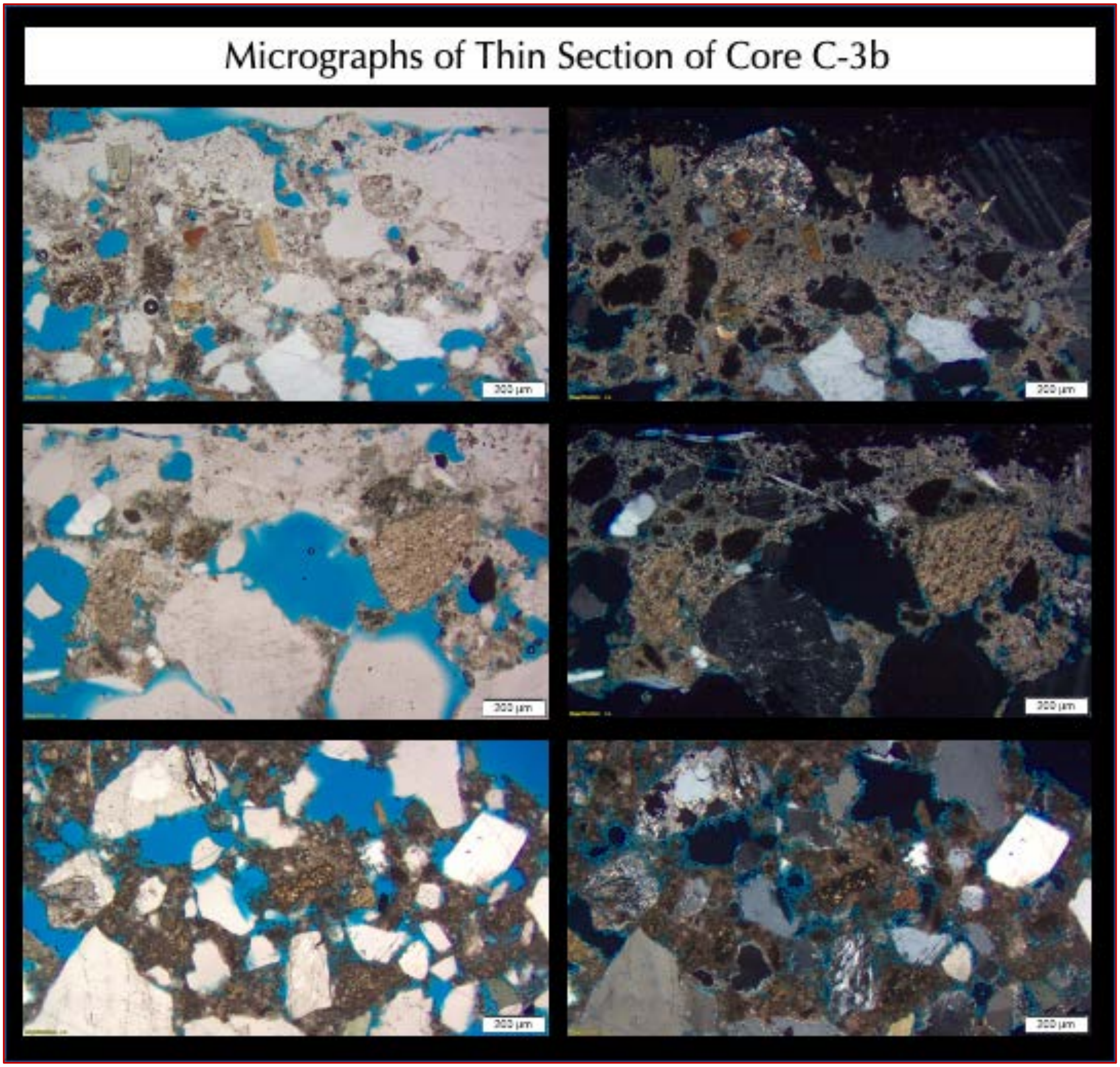

Figure 35: Micrographs of thin section of Core C-3b showing atmospheric carbonation of soft, porous paste at the exposed surface region, which is shown in the top and middle row photos, crushed limestone-dolomite coarse aggregate, natural siliceous (quartz, quartzite, quartz siltstone and sandstone), calcareous (limestone, dolomite), and argillaceous (shale) sand particles in fine aggregate, and Portland cement paste.

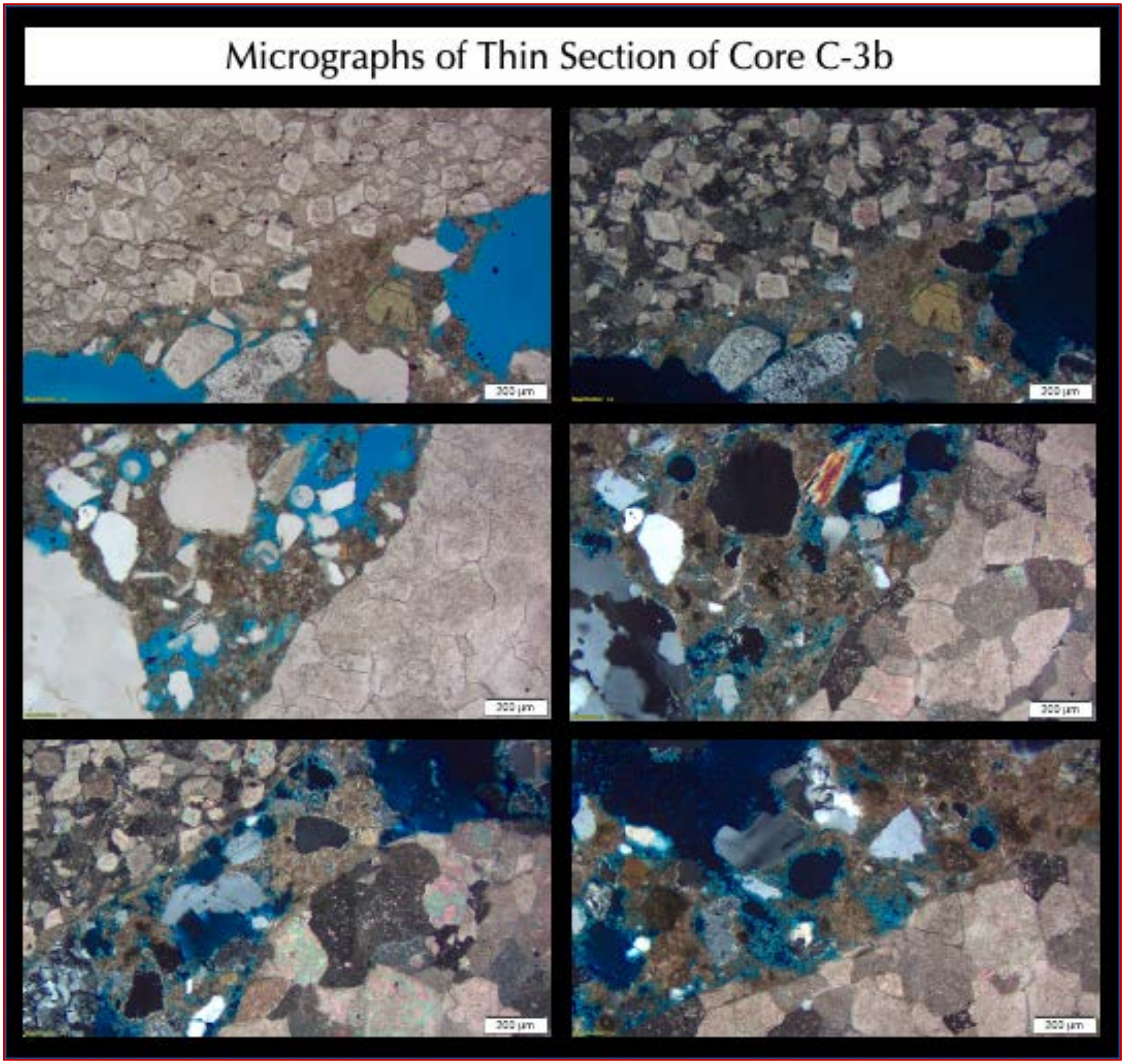

Figure 36: Micrographs of thin section of Core C-3b showing crushed limestone-dolomite coarse aggregate, natural siliceous (quartz, quartzite, quartz siltstone and sandstone), calcareous (limestone, dolomite) and argillaceous (shale) sand particles in fine aggregate, and Portland cement paste.

COARSE AGGREGATES

Coarse aggregates are compositionally similar crushed limestone and dolomite in both Cores C-2b and C-3b examined petrographically, but the particle size and grain size distribution are very different (e.g., see Figures 29 to 32), which for its volumetric dominance in concrete, has provided a significant influence on the properties and performance of concrete in these two cores.

For concrete in Core C-2b, crushed limestone/dolomite particles are mostly elongated, well-graded, and well-distributed where abundance of elongated particles has not only increased the water requirements of concrete but also created difficulty in effective filling of all interstitial spaces with the mortar fraction thereby leaving many coarse irregular-shaped entrapped voids between the particles and weak aggregate-mortar bonds due to inadequate consolidation and filling of particles with mortar fraction to the extent of creating a dry pack appearance of concrete. This has direct influence on the compressive strength, which showed only 1590 psi strength.

For concrete in Core C-3b, crushed limestone/dolomite coarse aggregate particles are not elongated as seen in C-2b, mostly equidimensional with only a few elongated, but poorly graded due to the deficiency of many finer and intermediate-size particles which has increased the mortar fraction of concrete significantly. Unlike concrete in Core C-2b, interstitial spaces between the crushed stone particles are effectively filled with mortar fraction without any very coarse voids. The mortar fraction itself, however, showed many coarse entrapped voids though not as coarse as the voids seen in Core C-2b and has soft, porous, high water-cement ratio paste, which are discussed later. High mortar fraction of poor quality mortar due to poor grading of crushed stone aggregates has affected the compressive strength, with only 1900 psi strength reported.

Crushed limestone particles in both cores are medium gray, dense, hard, angular, and massive mosaic textured which is typical of carbonate rocks. Limestone particles show medium to coarse grained texture, often with argillaceous veins, dolomite shows rhombic crystals of dolomite in matrix of calcite, and siliceous materials. Coarse aggregate particles in both cores are unaltered, uncoated, uncracked, and present in sound conditions. There is no evidence of alkali-aggregate reactions of coarse aggregate particles in the samples.

FINE AGGREGATES

Fine aggregates are compositionally similar natural siliceous-argillaceous sand in both cores with some fractions from crushed limestone/dolomite having a nominal maximum size of $^3/_8$ in. containing major amount of siliceous component (consisting of variably strained quartz and quartzite, feldspar, quartz siltstone and sandstone, etc.), and a minor to subordinate amount of argillaceous component (shale, argillaceous siltstone). Particles are variably colored, rounded to subangular, dense, hard, equidimensional to elongated, unaltered, uncoated, and uncracked. Fine aggregate particles are well-graded and well-distributed. There is no evidence of alkali-aggregate reaction of fine aggregate particles. Fine aggregate particles have been sound during their service in the concretes.

Properties and Compositions of Aggregates	C-2b	C-3b
Coarse Aggregates		
Types	Crushed Stone	Crushed Stone
Nominal maximum size (in.)	$^1/_2$ in. (12.5 mm)	$1^1/_4$ in. (31.75 mm)
Rock Types	Limestone, dolomite	Limestone, dolomite
Angularity, Density, Hardness, Color, Texture, Sphericity	Medium gray, dense, hard, angular, massive textured. Particles are mostly elongated in Core C-2b to mostly equidimensional to elongated in Core C-3b	
Cracking, Alteration, Coating	Unaltered, uncoated, and uncracked	Unaltered, uncoated, and uncracked
Grading & Distribution	Well-graded and Well-distributed	Poorly-graded and Well-distributed
Soundness	Sound	Sound
Alkali-Aggregate Reactivity	None	None
Fine Aggregates		
Types	Natural siliceous-argillaceous sand	Natural siliceous-argillaceous sand
Nominal maximum size (in.)	$^3/_8$ in. (9.5 mm)	$^3/_8$ in. (9.5 mm)
Rock Types	Major amount of siliceous component (consisting of variably strained quartz and quartzite, feldspar, quartz siltstone and sandstone, shale, etc.), and a subordinate amount of argillaceous component (shale, argillaceous siltstone)	
Cracking, Alteration, Coating	Variably colored, rounded to subangular, dense, hard, equidimensional to elongated	Variably colored, rounded to subangular, dense, hard, equidimensional to elongated
Grading & Distribution	Well-graded and Well-distributed	Well-graded and Well-distributed
Soundness	Sound	Sound
Alkali-Aggregate Reactivity	None	None

Table 2: Properties of coarse and fine aggregates of concrete cores.

PASTE

Properties and composition of hardened cement pastes are summarized in Table 2. Freshly fractured surfaces have subvitreous lusters and subconchoidal textures. Residual and relict Portland cement particles are present and estimated to constitute 6 to 8 percent of the paste volumes in the interiors.

Properties and Compositions of Paste	C-2b	C-3b
Color, Hardness, Porosity, Luster	Medium gray, soft, porous	Light gray to beige, soft, porous
Residual Portland Cement Particles	Normal, 6 to 8 percent by paste volume in the body but 20 to 30 percent at the top trowel-densified surface region	
Calcium hydroxide from cement hydration	Normal, 6 to 8 percent by paste volume	Normal, 6 to 8 percent by paste volume
Pozzolans, Slag, etc.	None	None
Water-cementitious materials ratio (*w/cm*), estimated	0.45 to 0.50 local variation	0.55 to 0.60
Cement Content (bags per cubic yard)	5 to $5^1/_2$	6 to $6^1/_2$

Properties and Compositions of Paste	C-2b	C-3b
Secondary Deposits	None	None
Depth of Carbonation, mm	Not present for middle portion of core	10 to 15 mm from exposed end thereafter patchy carbonation to a depth of 2 inches
Microcracking	Not found except shrinkage microcracks in paste from high water-cement ratio	
Aggregate-paste Bond	Weak	Moderately tight
Bleeding, Tempering	None	None
Chemical deterioration	None	None

Table 3: Proportions and composition of hardened cement paste.

AIR-VOID ANALYSES

Figures 25 through 28 show detailed air-void systems of concrete in micrographs of lapped cross sections of the Cores C-2b, 3b, 4b, and 6b viewed through a stereo-zoom microscope. Intentionally introduced fine, discrete, spherical or near-spherical less than 1 mm size entrained air voids are not detected in any core, but coarse (> 1 mm size), near-spherical to irregular-shaped entrapped voids are found in all cores, sometimes as high as 10 to 15 percent to give dry-pack appearance of concrete as in Core C-2b with a noticeable reduction in compressive strength of concrete to 1590 psi. Based on detailed air-void analyses of Cores C-4b and 6b, concrete in both cores are determined to be non-air-entrained having no evidence of addition of an air-entraining agent. The following Table provides the determined air-void parameters of concrete in the cores:

Air-void Systems and Parameters	C-4b	C-6b
Air-Void System	Non-Air-Entrained	Non-Air-Entrained
Total Air Content, %, Determined	2.91	4.91
Entrained Air Content, %, Determined	0.47*	0.96*
Paste Content, %, Determined	19.17	28.39
Paste-Air Ratio	6.581	5.784
Specific Surface, in.^{2}/in.^{3}	191	256
Air-Void Spacing Factor, in.	0.0275	0.0194

Table 4: Properties and parameters of air-void system of concretes in the cores. Entrained air-voids are defined as discrete, spherical or near-spherical voids of sizes 1 mm or less. Common industry (e.g., ACI, ASTM) requirements for a concrete containing $^1/_2$ in. nominal maximum size coarse aggregate and exposed to a moist outdoor environment of cyclic freezing and thawing are an air content of 7.5±1$^1/_2$ percent, a minimum air-void specific surface of 600 in.^{2}/in.^{3}, and a maximum void-spacing factor of 0.008 in. *For entrained void calculations though these voids occurred as small spherical voids of less than 1 mm size, but they are actually entrapped voids.

Air occurs as coarse, near-spherical and irregularly shaped voids of sizes coarser than 1 mm that are characteristic of entrapped air. Air-void systems of concrete are suggestive of no intentional addition of an air-entraining agent in the mix. The total air contents are determined to be 2.9 to 4.9 percent which are all coarse, irregular-shaped entrapped air. The specific surface of air-void systems, which measure the fineness of air voids are measured to be

200 to 260 in.^{2}/in.^{3} and the air-void spacing factors, which measure closeness of air bubbles are measured to be 0.0194 to 0.0275 inch. Air-void parameters indicate non-air-entrained concretes as seen in Figures 27 and 28.

WATER-SOLUBLE CHLORIDE AND SULFATE CONTENTS

Core ID & Depth of Sample Section		Water-Soluble Chloride & Sulfate Contents from Ion Chromatography		
		% Chloride by mass of concrete	% Chloride by mass of cement (assuming 15% cement in normal-weight concrete)	Water-soluble Sulfate
C-1b	3″ from face	0.0051	0.034	0.0740
	12.5″ from face	0.0025	0.016	0.0563
C-2b	3″ from face	0.0049	0.032	0.0578
	13.25″ from face	0.0027	0.018	0.0877
C-3c	3″ from face	0.0379	0.252	0.0461
	12″ from face	0.0287	0.191	0.0419
C-3d	3″ from face	0.0032	0.021	0.1390
	14.5″ from face	0.0021	0.014	0.0688
C-6b	3″ from face	0.0037	0.024	0.0390
	12.75″ from face	0.0012	0.008	0.0370

Table 5: Water-soluble chloride and sulfate contents. Chloride results for most cores are less than the common industry-recommended maximum threshold limit of 0.20 percent chloride by mass of cement to cause corrosion of steel in concrete in the presence of oxygen and moisture.

Table 5 and Figures 37 to 41 show results of water-soluble chloride and sulfate contents of concrete determined from ion chromatography (*a la* ASTM D 4327) on pulverized sections from the marked locations at 3 in. and interior (12 in. to 14.5 in.) depths. All cores show evidence of detectable but negligible chloride and sulfate at the 3 in. and interior depths, which are indicative of lack of any chloride or sulfate exposure from the environment, which is consistent with the reported mild enclosed environment of train shed. Core C-3c showed the highest chloride content of all though still not excessively higher than the common industry-recommended threshold chloride limit of 0.20 percent chloride by mass of cement for chloride-induced corrosion of steel in concrete to occur in the presence of oxygen and moisture.

Sulfate contents are all within the values anticipated for contributions only from the Portland cement paste except the fact that the sulfate results are noticeably lower than the values for a concrete containing 15 percent Portland cement by mass (in which case sulfate content should have been 0.45 percent by mass of concrete containing 15 percent Portland cement where cement has sulfate content of 3 percent by mass), indicating use of lower-then-normal cement content in the cores, which is also indicative of the low compressive strength results reported.

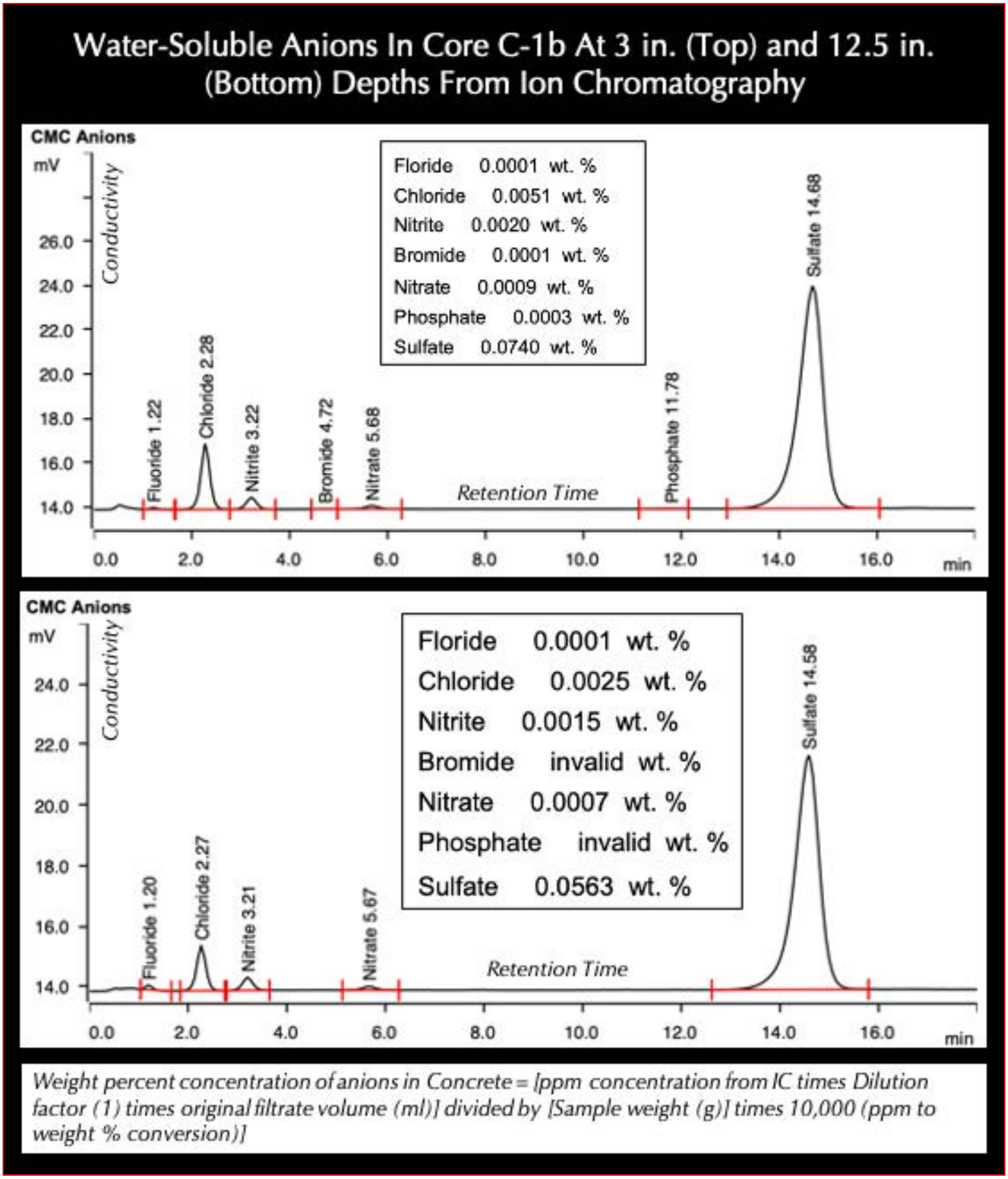

Figure 37: Ion chromatograms of water-soluble anions of filtrates from the 3 in. and 12.5 in. depths of Core C-1b showing negligible chloride and sulfate ions at the exposed and interior concrete with slightly lesser values from the interior. Results are indicative of the lack of any external exposures to chloride or sulfate salts during service, which is consistent with its reported mild exposure of interior train shed location of core.

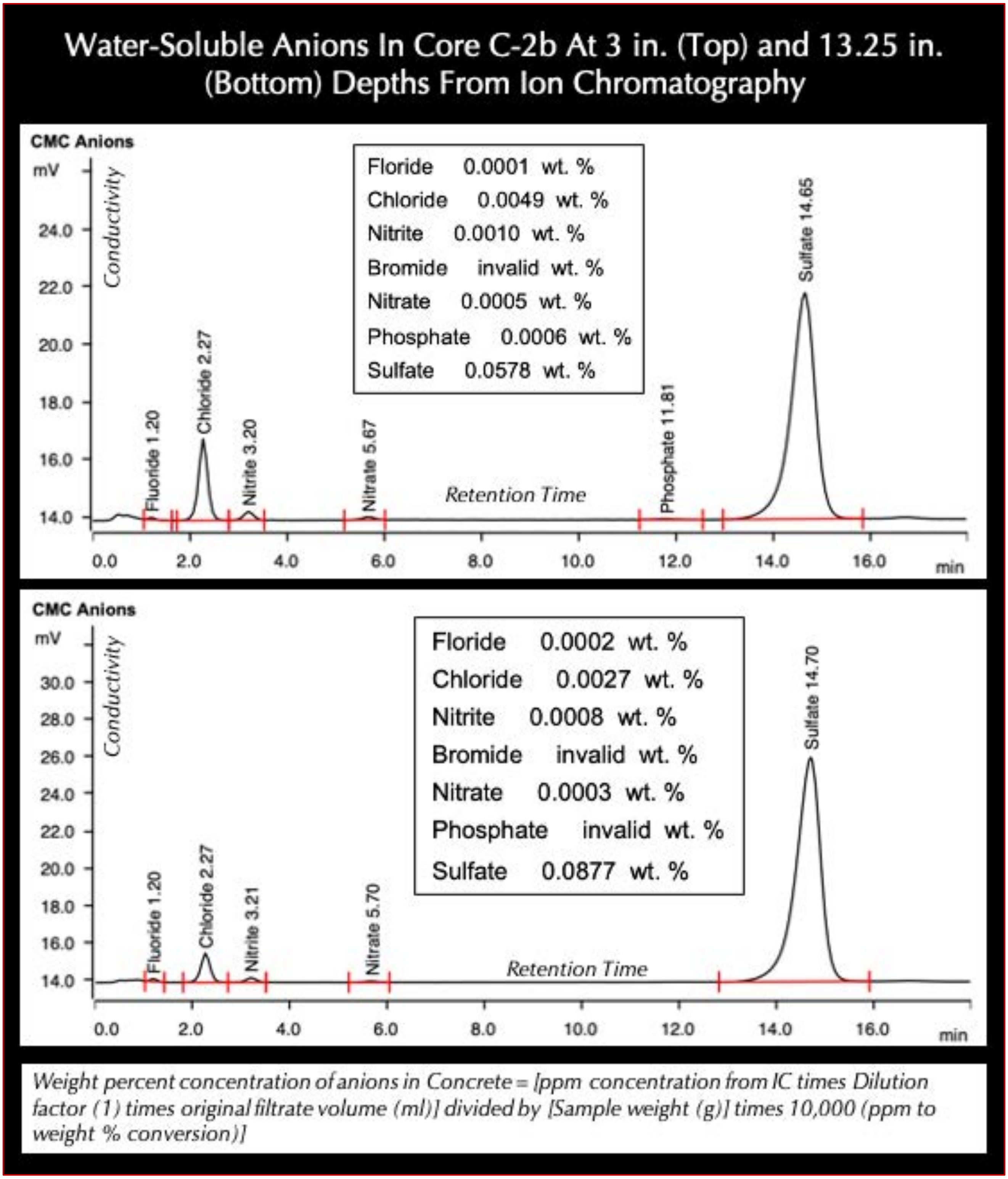

Figure 38: Ion chromatograms of water-soluble anions of filtrates from the 3 in. and 13.25 in. depths of Core C-2b showing negligible chloride and sulfate ions at the exposed and interior concrete with slightly lesser values from the interior. Results are indicative of the lack of any external exposures to chloride or sulfate salts during service, which is consistent with its reported mild exposure of interior train shed location of core.

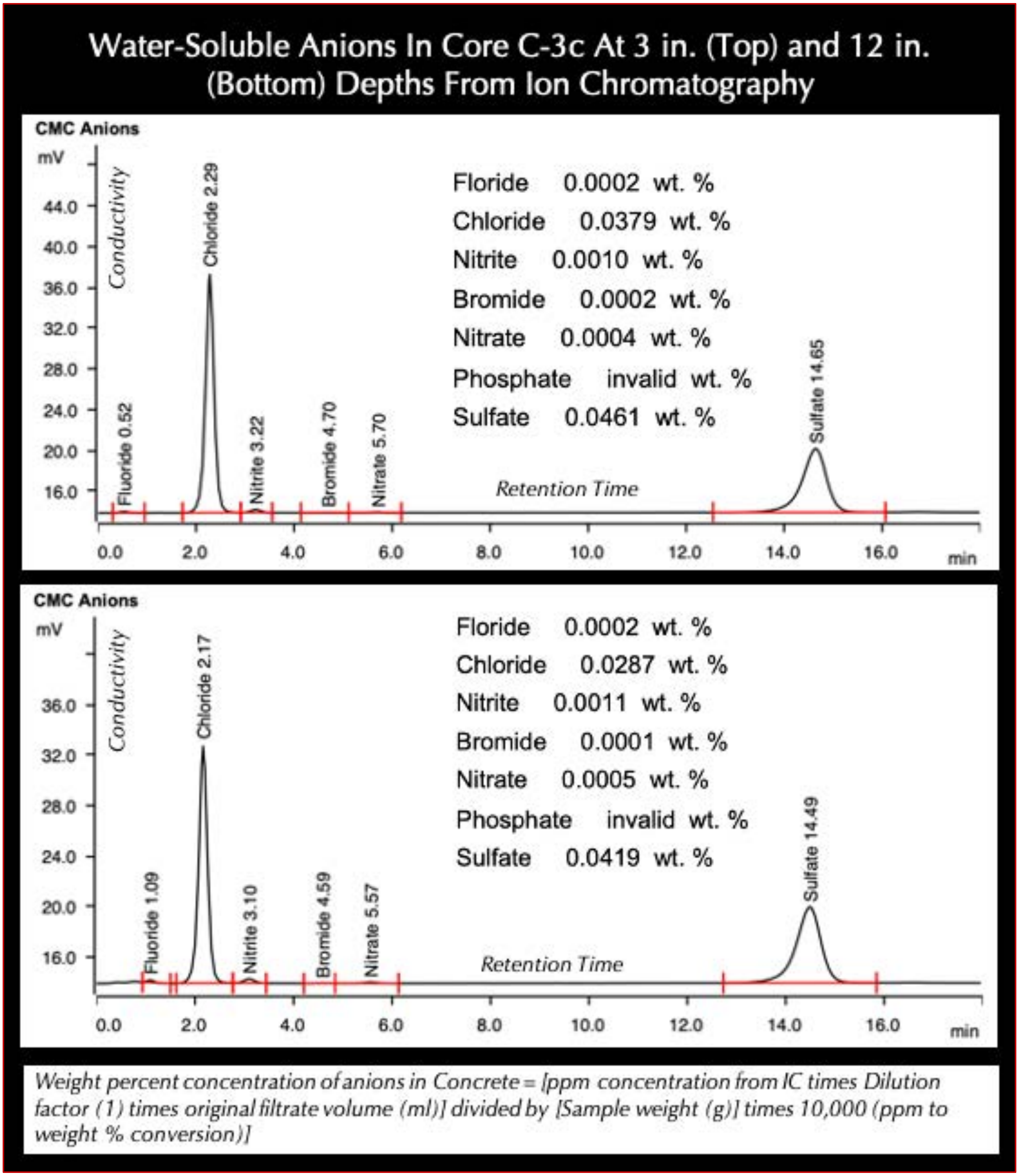

Figure 39: Ion chromatograms of water-soluble anions of filtrates from the 3 in. and 12 in. depths of Core C-3c showing detectable chloride and negligible sulfate ions at the exposed and interior concrete with slightly lesser values from the interior. Results are indicative of a potential external exposure to chloride during service, but at mild scale, which is consistent with its reported mild exposure of interior train shed location of core.

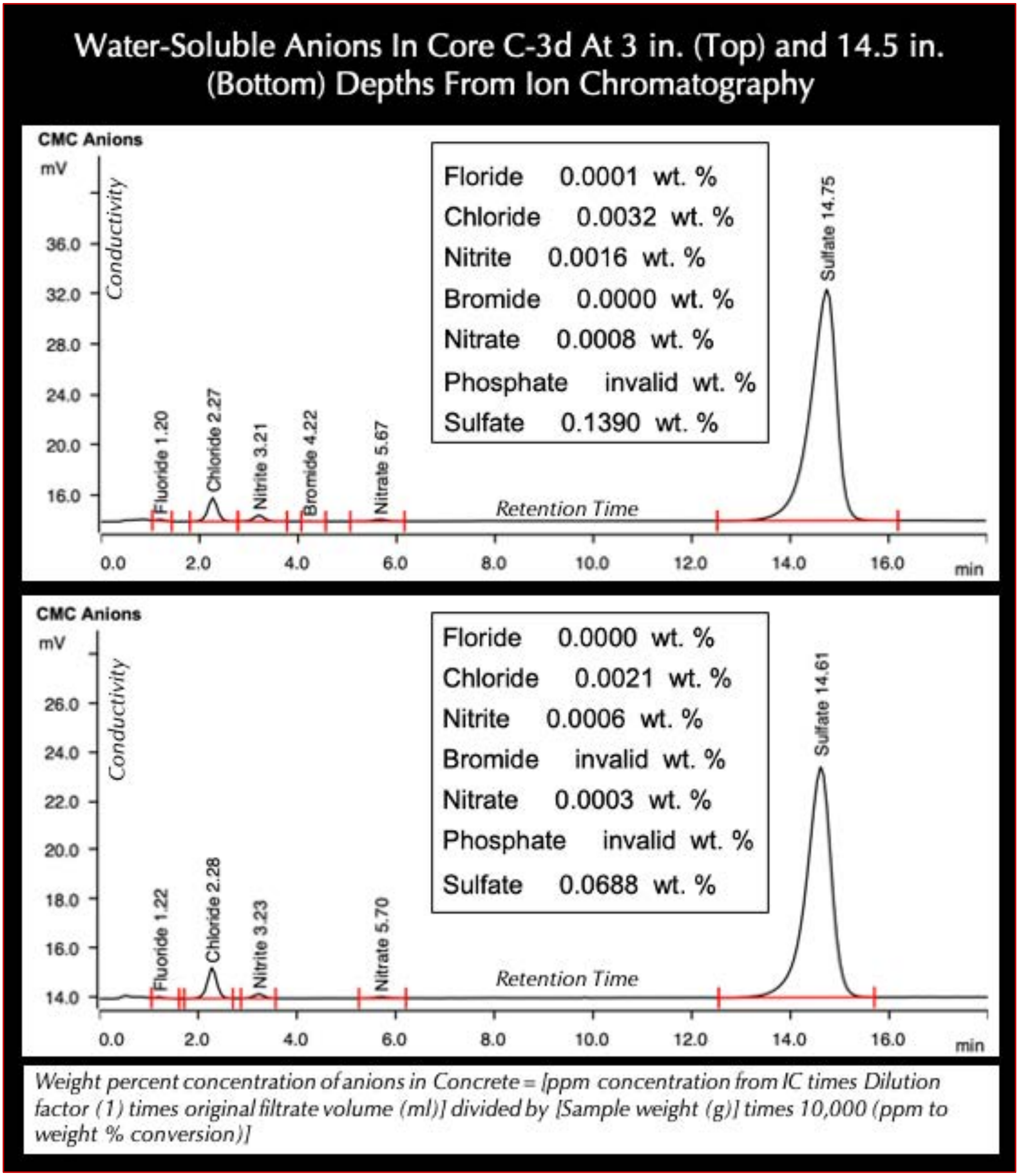

Figure 40: Ion chromatograms of water-soluble anions of filtrates from the 3 in. and 14.5 in. depths of Core C-3d showing negligible chloride and sulfate ions at the exposed and interior concrete with slightly lesser values from the interior. Results are indicative of the lack of any external exposures to chloride or sulfate salts during service, which is consistent with its reported mild exposure of interior train shed location of core.

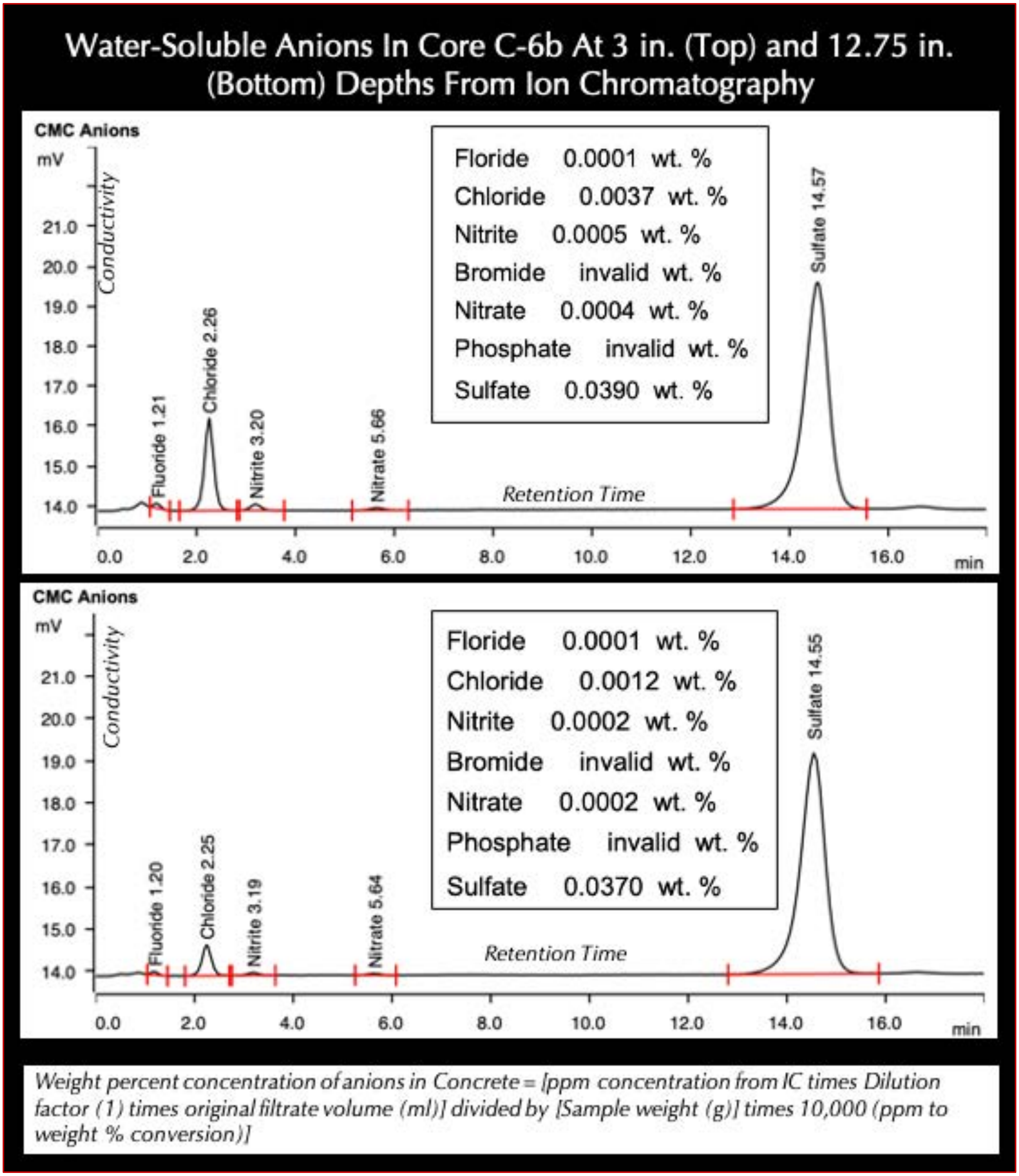

Figure 41: Ion chromatograms of water-soluble anions of filtrates from the 3 in. and 12.75 in. depths of Core C-6b showing negligible chloride and sulfate ions at the exposed and interior concrete with slightly lesser values from the interior. Results are indicative of the lack of any external exposures to chloride or sulfate salts during service, which is consistent with its reported mild exposure of interior train shed location of core.

COMPRESSIVE STRENGTH RESULTS

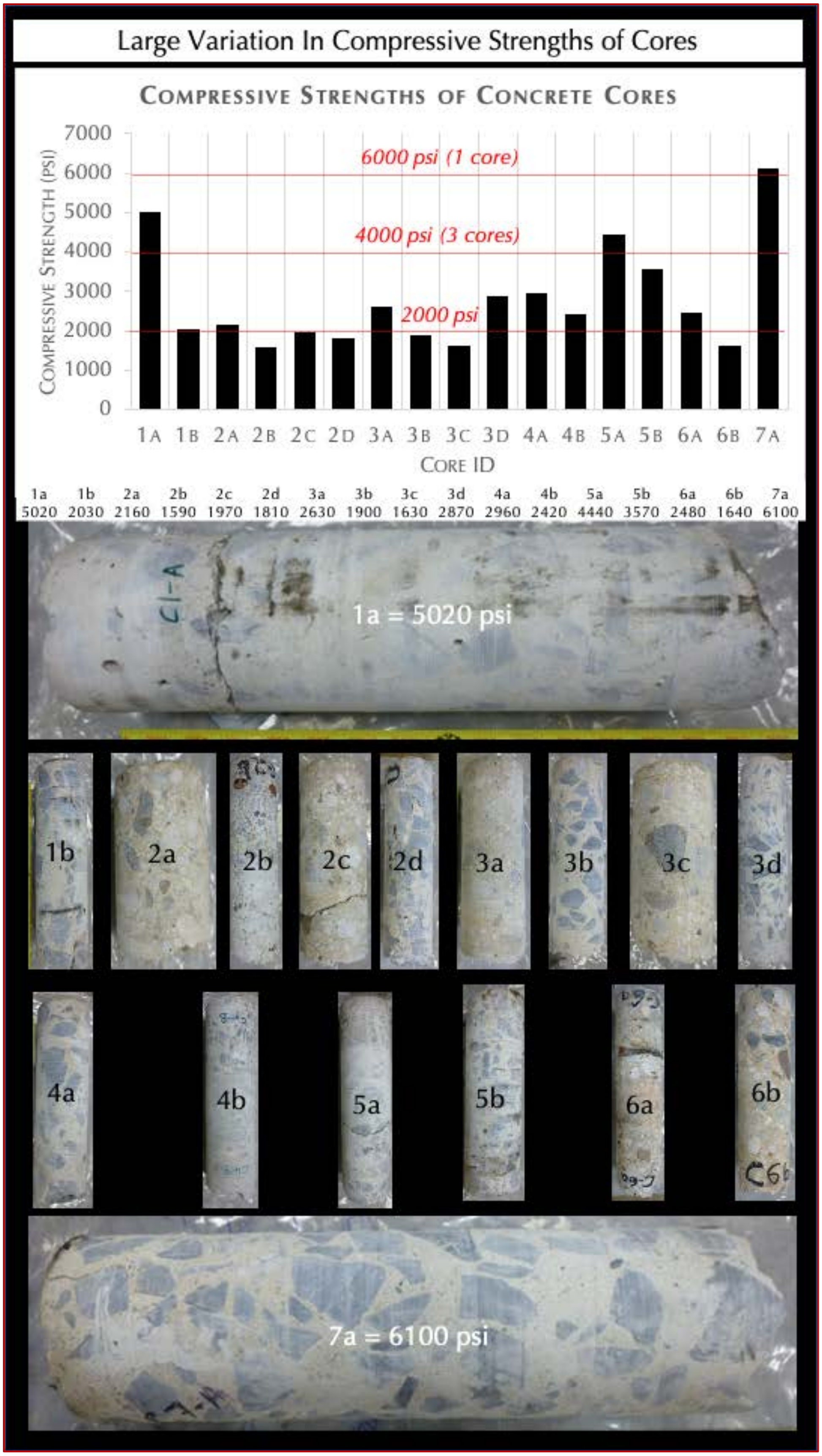

Figure 42: Results of compressive strengths of all cores provided.

Results show large variations in strength, e.g., from as low as 1590 psi to 6100 psi, which is indicative of large variations in compositions, qualities, and conditions of concrete tested.

Of 17 cores tested, only one core provided strength in excess of 6000 psi (Core C-7a), two cores including C-7a provided results in excess of 4000 psi (Cores C-1a and 5a), whereas 13 other cores provided very low strengths around 2000 psi, which is judged to be due to their inherent soft, porous, high water-cement ratios of paste.

Low strength due to poor quality of paste and inadequate consolidation of concrete are seen in two cores (Core C-2b and 3b) tested by petrographic examinations, which showed strength results of only 1590 psi, and 1900 psi where low strength in Core C-2b is due to abundant coarse entrapped voids due to inadequate consolidation of coarse aggregate by the mortar fraction, whereas low strength in Core C-3b is due to soft, porous, high water-cement ratio of paste despite good consolidation.

DISCUSSIONS

SIMILARITIES AND VARIATION IN CONCRETE COMPOSITIONS

Results obtained from petrographic examinations of two cores, air-void analysis of two other cores, and water-soluble chloride and sulfate analyses of five cores at two different depths for each core, along with reported compressive strength results show some similarities as well as differences in the concrete delivered to the core locations, which may indicate multiple repair and rehabilitation events to the original 1910's construction.

Coarse aggregates used in most of the cores are either crushed limestone-dolomite (e.g., in Cores C-1a, 1b, 2b, 3a, 3b, 3d, 4a, 5a, 5b, and 7a), or crushed gravel (e.g., in Cores C-2a, 2c, 3c, 6a, 6b) where crushed limestone/dolomite used in the former series of cores are compositionally similar to each other indicating their derivation from same or similar source, and also crushed gravel in the second series of cores are also compositionally similar to each other again indicting their derivation from similar source. Core C-4b has crushed granite, which is different from the other ones.

Despite compositional similarities of crushed limestone-dolomite, however, grain size, shape, and distribution of crushed limestone as well as the proportions of crushed stone to the mortar fractions of concrete varied considerably between the cores of first series, indicating different crushing operations despite their compositional similarities, which has provided a strong influence on the properties and performance of these concretes. For concrete in Core C-2b, crushed limestone/dolomite particles are mostly elongated, well-graded, and well-distributed where abundance of elongated particles has not only increased the water requirements of concrete but also created difficulty in effective filling of all interstitial spaces with the mortar fraction thereby leaving many coarse irregular-shaped entrapped voids between the particles and weak aggregate-mortar bonds due to inadequate consolidation and filling of particles with mortar fraction to the extent of creating a dry pack appearance of concrete. This has direct influence on the compressive strength, which showed only 1590 psi strength. For concrete in Core C-3b, crushed limestone/dolomite coarse aggregate particles are not elongated as seen in C-2b mostly equidimensional with only a few elongated, but poorly graded due to the deficiency of many finer and intermediate-size particles which has increased the mortar fraction of concrete significantly. Unlike concrete in Core C-2b, interstitial spaces between the crushed stone particles are effectively filled with mortar fraction without any very coarse voids. The mortar fraction itself, however, showed many coarse entrapped voids though not as coarse as the voids seen in Core C-2b and has soft, porous, high water-cement ratio paste, which are discussed later. High mortar fraction of poor quality mortar due to poor grading of crushed stone aggregates has affected the compressive strength, with only 1900 psi strength reported.

Fine aggregate in all cores are compositionally similar natural siliceous-argillaceous rocks indicating derivation from similar source.

Pastes are Portland cement based at least in two cores examined by petrography, i.e., in Cores C-2b and 3b with no evidence of any pozzolanic or cementitious materials.

Concretes in four cores examined by petrography (Cores C-2b and 3b) and air-void analysis (C-4b, and 6b) are all non-air-entrained with no indication of addition of any air entraining chemical.

Perhaps the most startling evidence of variations in compositions, qualities, and conditions of concrete came from large variations in strength results provided, e.g., from as low as 1540 psi to as high as 6100 psi where only one out of 17 cores tested showed strength above 6000 psi, three (except the > 6000 psi core) showed strength above 4000 psi, whereas 13 other cores showed strengths around 2000 psi. Such overall low compressive strengths of majority of the cores tested indicate overall poor quality of concrete.

Since no distress is reported for the concrete largely due to their location in a protected or covered environment of train shed, where the typical harsh weather condition of New York from exposures to moisture to cyclic freezing and thawing to chloride containing deicing chemicals may not have reached the concrete to affect the long-term durability. Based on overall poor quality of concrete found from this study, the need to keep the concrete protected from the environment especially after finding their lack of air entrainment to affect freeze-thaw durability and lack of adequate industry-recommended compressive strength of at least 4500 psi in the moist outdoor environment to affect both durability and long-term performance. Intermittent exposure to moisture and salt from trains passing by can bring some distress due to low strength and lack of air unless the concrete remains undersaturated during its service to prevent any freezing-related stress to develop. Abundant entrapped air despite lack of entrained air may in fact provide some benefit in providing rooms to accommodate frozen water and prevent freezing-related cracking or spalling.

All cores show evidence of detectable but negligible chloride and sulfate at the 3 in. and interior depths, which are indicative of lack of any chloride or sulfate exposure from the environment, which is consistent with the reported mild enclosed environment of train shed. Core C-3c showed the highest chloride content of all though still not excessively higher than the common industry-recommended threshold chloride limit of 0.20 percent chloride by mass of cement for chloride-induced corrosion of steel in concrete to occur in the presence of oxygen and moisture. Sulfate contents are all within the values anticipated for contributions only from the Portland cement paste except the fact that the sulfate results are noticeably lower than the values for a concrete containing 15 percent Portland cement by mass (in which case sulfate content should have been 0.45 percent by mass of concrete containing 15 percent Portland cement where cement has sulfate content of 3 percent by mass), indicating use of lower-then-normal cement content in the cores, which is also indicative of the low compressive strength results reported.

REFERENCES

ASTM C 856 "Standard Practice for Petrographic Examination of Hardened Concrete," Vol. 4.02, ASTM International, West Conshohocken, PA, 2014.

ASTM C 457 "Standard Test Method for Microscopical Determination of Parameters of the Air-Void System in Hardened Concrete," Vol. 4.02, ASTM International, West Conshohocken, PA, 2016.

ASTM C 1218 "Standard Test Method for Water-Soluble Chloride in Mortar and Concrete," Vol. 4.02, ASTM International, West Conshohocken, PA, 2017.

ASTM D 4327, "Standard Test Method for Anions in Water by Suppressed Ion Chromatography," Vol. 11.01, ASTM International, West Conshohocken, PA, 2019.

Jana, D., and Cole, A.A., "Microscopy: A Practical Solution to Concrete Problems," Bulletin of Concrete Industry Board, September 1997, pp. 18-22.

Jana, D., "Petrography: A Powerful Tool For Solving Common Concrete Problems," Civil Engineering NEWS, March 1997, pp. 40-44.

Jana, D., "Sample Preparation Techniques in Petrographic Examinations of Construction Materials: A State-of-the-art Review," Proceedings of the 28th Conference on Cement Microscopy, International Cement Microcopy Association, Denver, Colorado, pp. 23-70, 2006.

Jana, D., "Concrete, Construction, or Salt – Which Causes Scaling? Part 2: Importance of Finishing Practices"; Concrete International, December 2004, pp. 51-56, American Concrete Institute.

Jana, D., "Petrography and Concrete Repair – A Link is Needed," Point of View Publication in Concrete International, American Concrete Institute, pp. 37-39, January 2005.

✪ ✪ ✪ END OF TEXT ✪ ✪ ✪

END OF REPORT[1]

[1] The CMC logo is made using a lapped polished section of a 1930's concrete from an underground tunnel in the U.S. Capitol.